AN INVESTIGATION OF MICROSTRUCTURE AND MECHANICAL PROPERTIES OF ALUMINUM MATRIX COMPOSITE REINFORCED WITH B_4C PARTICULATES MANUFACTURED BY POWDER METALLURGY METHOD

By
Lütfiye Feray GÜLERYÜZ

Submitted to the Institute of Graduate Studies in
Science and Engineering in partial fulfillment of
the requirements for the degree of
Master of Science
in
Mechanical Engineering

Yeditepe University
April 2010

AN INVESTIGATION OF MICROSTRUCTURE AND MECHANICAL PROPERTIES OF ALUMINUM MATRIX COMPOSITE REINFORCED WITH B_4C PARTICULATES MANUFACTURED BY POWDER METALLURGY METHOD

APPROVED BY:

Asst. Prof. Dr. Namık CIBLAK …….
(Thesis Supervisor)

Asst. Prof. Dr. A. Fethi OKYAR ……..

Asst. Prof. Dr. Deniz UZUNSOY ……..

DATE OF APPROVAL: / / 2010

Dedicated to my father, KEMAL ÖZBİLEN

ACKNOWLEDGEMENTS

I would like to thank to my advisor Asst. Prof. Dr. Namık ÇIBLAK for his continuous support, ambition and patience during the study. My special gratitude goes to Prof. Dr. Rasim İPEK for his contribution to the project. I especially thank to Asst. Prof. Dr. Deniz UZUNSOY for everything. This thesis would not have been possible without her contribution.

I am indebted to all of my colleagues who helped me directly or indirectly in preparing this project. Furthermore, I wish to thank Yildiz Technical University Central Laboratory; and Siemens, Borsen and Kosgeb laboratories for their cooperation. I also thank to Eti Maden Company for their help in obtaining B_4C powder.

Finally, I would like to thank to my family for their encouragement.

ABSTRACT

AN INVESTIGATION OF MICROSTRUCTURE AND MECHANICAL PROPERTIES OF ALUMINUM MATRIX COMPOSITE REINFORCED WITH B_4C PARTICULATES MANUFACTURED BY POWDER METALLURGY METHOD

Currently some composite materials, especially aluminum metal matrix composites with particulate reinforcement and related manufacturing methods are among important research topics because of their low density, high specific stiffness and specific strength, and, high wear resistance. Therefore, there exists a need for investigation of their mechanical properties and microstructures.

In this study, microstructure and physic mechanical properties of Al-B_4C composites, boron carbide (B_4C) particulate reinforcements in 63-μm diameter aluminum matrix, sintered at 550 ºC, are studied. The effects of parameters such as reinforcement particulate size and reinforcement percentage on hardness, compression strength, and microstructure are investigated.

Different sizes (22, 77, and 120-μm) and different amounts (3, 6, and 9 wt%) of B_4C were added to the base material, and pressureless sintering was conducted at 550 ºC under argon atmosphere. Resulting microstructures, densities, and compression test behaviors are studied.

It is observed that particle sizes and percentages of the reinforcement significantly influence the compression strength and hardness values. Visual inspection using SEM (Scanning Electron Microscope) analyses indicates that the microstructure of the composite is also greatly effected by these parameters. In addition, EDS (Energy Dispersive X-Ray Spectroscopy) and X-Ray Diffraction analyses were performed for reliable determination of the chemical composition.

ÖZET

TOZ METALURJİSİ YÖNTEMİYLE ÜRETİLEN BOR KARBÜRLE TAKVİYE EDİLMİŞ ALÜMİNYUM MATRİSİN MİKRO YAPISI VE MEKANİK ÖZELLİKLERİNİN İNCELENMESİ

Son zamanlarda partikül takviyeli alüminyum metal matris kompozitler yüksek mukavemet, düşük yoğunluk ve yüksek aşınma direncinden dolayı önemli araştırma konu başlıklarının arasına katılmıştır. Bundan dolayı, bu kompozitlerin mekanik özelliklerinin ve mikro yapılarının testlerle araştırılmasına gerek duyulmaktadır.

Bu çalışmada 550 ºC'de sinterlenmiş, bor-karbür (B_4C) takviyeli 63-µm çaplı alüminyum toz matrisinden elde edilmiş olan alüminyum bor-karbür kompozitlerin (Al-B_4C) mikro yapıları ve mekanik özellikleri çalışılmıştır. Takviye partikül büyüklüğü ve takviye yüzdesinin yüzey sertlik, basma dayanımı, ve mikro yapı üzerindeki etkileri incelenmiştir.

Değişik partikül boyutlarında (22, 77, and 120-µm) ve değişik kütle yüzdelerinde (3, 6, and 9) B_4C aliminyum matrise eklenip, 550ºC argon atmosferinde sinterlenmiştir. Bunların sonucunda elde edilen mikro yapılar, yoğunluk, ve basma testi davranışları çalışılmıştır

Takviye parça büyüklüklerinin ve yüzdelerinin basma dayanımını ve sertlik değerleri üzerinde önemli oranda etkili olduğu gözlenmiştir. SEM (Taramalı Elektron Mikroskobu) analizleri kompozitlerin mikro yapılarının da bu parametreler tarafından etkilendiğini göstermiştir. Ayrıca, kimyasal kompozisyonun güvenilir bir biçimde belirlenmesi amacıyla EDS (Enerji Dağılım Spektroskopisi) ve X-Işını kırınımı analizleri de yapılmıştır

TABLE OF CONTENTS

LIST OF FIGURES

LIST OF TABLES

LIST OF SYMBOLS/ABBREVIATONS

Al	Aluminum
E	Modulus of elasticity (Young's modulus)
Mg	Magnesium
MPa	Pascal
Si	Silicon
Ti	Titanium
wt%	Weight percent
Zn	Zinc
μm	Micrometer
ν	Poisson's ratio
σ	Engineering stress
EDS	Energy Dispersive Spectrum
EPMA	European Powder Metallurgy Association
HB	Brinell hardness
MMC	Metal matrix composite
MPIF	Metal Powder Industries Federation
P/M	Powder Metallurgy
SEM	Scanning electron microscop

1. INTRODUCTION

It is a fact that technological development depends on advantages in the field of materials. The idea of composite materials is not a new or recent one. Nature is full of examples. Wood is a fibrous composite, cellulose fiber in a lignin matrix. The cellulose fibers have high tensile strength but are very flexible (low stiffness) while the lignin matrix joins the fibers and furnishes the stiffness. Bone is another example of natural composite that supports the weight of various members of body [1].

Recently, Metal matrix composites (MMCs) have been widely investigated and applied. MMCs are a class of materials which can be designed to combine the strength, ductility and formability of metallic alloys with the nonmetallic compounds such as silicon carbide, aluminum oxide, boron carbide, etc. The definition of MMCs is at least two or more materials are combined on a microscopic scale to form a useful third material. The reinforcements can be discontinuous, in the shape of sphere, irregular rounded or whiskers or they can be continuous fibers. MMCs offer better opportunities to provide combinations of physical and mechanical properties not achievable in monolithic alloys. These properties are, strength, stiffness, corrosion resistance, wear resistance, weight, thermal conductivity, fatigue life, acoustical insulation, etc.

Composite materials are ideal for structural applications where high strength-to-weight and stiffness-to-weight rations are required aircraft and spacecraft. They are typical weight sensitive structures in which composite materials are effective. The study of composite materials actually has many topics such as manufacturing processes, elasticity, strength of materials and micromechanics [2]. The objective of this study to introduce of the mechanical behavior of composite and microstructure materials.

While MMCs have been used for many years the field has a great potential to be applied in automobile and aerospace industries because of their high specific tensile, strength and modulus, high wear resistance [3].

There are several methods to fabricate MMCs. Powder metallurgy technique has been the traditional method of manufacturing MMC materials and components. P/M has the ability to fabricate high quality, complex parts to close tolerances in an economical method. The basic P/M takes a metal powder with specific characteristic of size, shape, and density then converts it into a strong, high performance shape. P/M steps include the compaction of the powder and sintering. The process effectively uses automated operations with low energy consumption, high benefit and low costs. Further, powder metallurgy is a flexible manufacturing process capable new materials, microstructures and properties.

Aluminum metal matrix composites with B_4C particulate reinforced investigate because of their low density, high specific stiffness and specific strength. So in this thesis their mechanical properties tested.

This thesis is scientifically organized in 5 chapters as follows:

The opening chapter, chapter 1 guides readers to the motivation and scope of this research work and chapter 1 includes composites and powder metallurgy and powder-PM aluminum, Includes, brief history general features physical properties advantageous and disadvantageous, and fields of applications.

Chapter 2 provides the literature survey applications of aluminum and its alloys, the criteria of selecting the matrix material and reinforcements. It also provides the basis of choosing the processing methods for this research work.

Chapter 3 presents information on materials used in this project and the art of preparing and arranging reinforcements in the matrix during processing stage and experimental studies. These shows microstructural, mechanical properties exhibited by Al-B_4C particles by PM. Experimental methodologies for different amounts of B_4C were added to the base material and sintering was conducted at 550 °C under argon atmosphere microstructure and hardness, density evolution ,compressing tests carried out in this project are also be described.

Chapter 4 presents the experimental results and discussion of Al matrix system. The addition of B_4C into Aluminum led to great improvement in strengths, hardness over the monolithic aluminum.

Chapter 5 presents the conclusions obtained from Al-B_4C system. Results exhibit that mechanical properties of pure aluminum are significantly increased as a result of simultaneous addition of B_4C particulates .The results show great potential of these composites in strength based engineering applications. Also in the last chapter 5 the main conclusions from the present study are listed and recommendations for the future work are prepared.

1.1. COMPOSITES

The word composite is the term composite material signifies that two or more materials are combined on a microscopic scale to form a useful third material. The key is the macroscopic examination of a material wherein the components can be identified by the naked eye. Different materials can be combined on microscopic scale such as in alloying of metals, but the resulting material is for all practical purposes, macroscopically homogeneous i.e. the components can be distinguished by the naked eye and essentially act together [2].

1.1.1. General Features of Composite Material

The advantage of composite materials is that, if well designed, they usually exhibit the best qualities of their components or constituents and often some qualities that neither constituent possesses.

Some of the properties that can be improved by forming a composite material are,

- Stiffness
- Strength
- Corrosion resistance

- Wear resistance
- Attractiveness
- Weight
- Fatigue life
- Temperature-dependant behavior
- Thermal insulation
- Thermal conductivity
- Acoustical insulation

1.1.2. Classification and Characteristics of Composite Materials

Many composite materials are composed of just two phases; one is termed as the matrix, and the other is called the dispersed phase. The matrix is continuous and surrounds the dispersed material Figure 1.1.

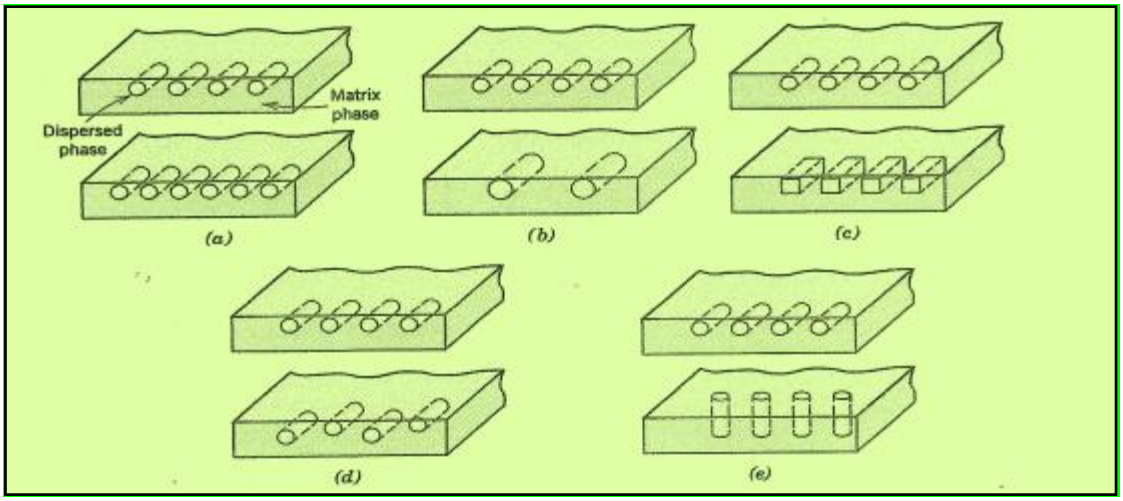

Figure 1.1. Schematic representations of the dispersed phase [4]

In this shape the composites are classified into three main divisions. Particle-reinforced, fiber-reinforced, and structural composite also least two subdivisions exist for [4].

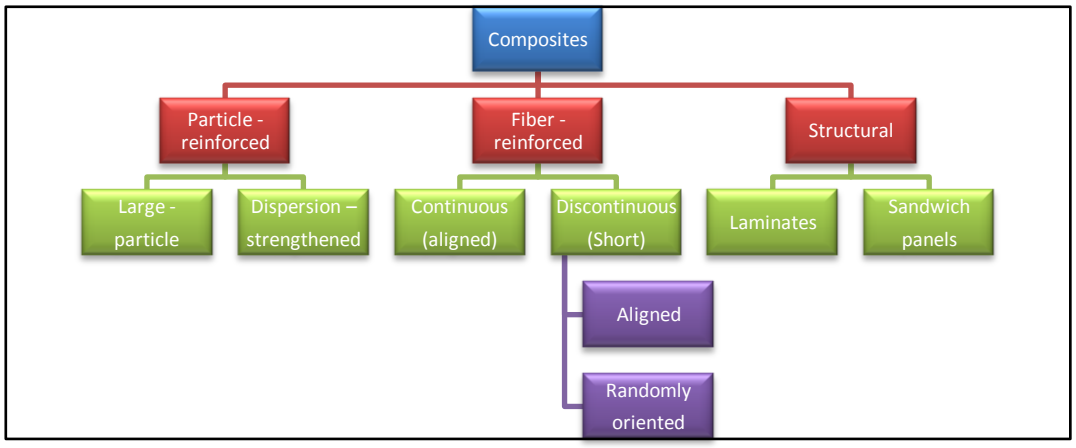

Figure 1.2. A classification scheme for composites [2]

1.1.3. Reinforcements

Reinforcements can be divided into two major groups. One is in the form of particles, flakes, whiskers. Whereas in the other form is fibrous. It turns out that most reinforcements used in composites have fibrous forms because resulting materials are stronger and stiffer. Another advantage in this case is its low cost. Cellulosic fibers in the form of cotton, flax, jute, hemp, sisal and ramie, have been used in textile industry, while wood and straw have been used in the paper industry. Glass fiber in various forms has been the most common reinforcement for polymer matrices [1].

Other high-performance fibers that combine high strength with high stiffness are boron, silicon carbide; carbon and alumina. These were all developed in the second part of the twentieth century [1].

Table 1.1. Typical reinforcements used in metal matrix composites [5]

Type	**Aspect Ratio**	**Diameter, μm**	**Examples**
Particle	1--4	1--25	SiC, Al_2O_3, BN, B_4C, WC
Short fiber or whisker	10--10000	1—5	C, SiC, Al_2O_3 Al_2O_3+SiO_2
Continuous fiber	>1000	3--150	SiC, Al_2O_3, C, B, W, Nb-Ti, Nb3Sn

1.1.4. Matrix Materials

In general metals and polymers are used as matrix materials, because some ductility is desirable; for ceramics-matrix composites the reinforcing component is added to improve fracture toughness [4].

Matrix materials are divided three main groups; these are polymer matrix composites, ceramic matrix composites and metal matrix composites.

Polymer matrix composites consist of a polymer resin (The term resin is used to denote a high-molecular-weight reinforcing) plastic as the matrix with fiber a reinforcement [4].

Ceramic Matrix Composites' main advantages of adding ceramic fibres to ceramics are very brittle and even a small increase in toughness may be advantageous [6].

Metal Matrix Composites (MMCs) is a ductile metal. These materials may be utilized at higher service temperatures than their base metal counter parts. Furthermore, the reinforcement may improve specific stiffness, specific strength, abrasion resistance, creep resistance, thermal conductivity and dimensional stability. Some of the advantages of these materials over the polymer-matrix composites include higher operating temperature, nonflammability and greater resistance to degradation by organic fluids [4].
The metal matrix composite is much more expensive than polymer matrix composites and therefore their (MMC) use is somewhat restricted.

The super alloys as well as alloys of aluminum, magnesium, titanium and copper are employed as matrix materials. The reinforcement may be in the form of particles, both continuous and discontinuous fibers and whiskers. Concentrations normally range between 10 and 60 volume %. Continuous fiber materials include carbon, silicon carbide, boron aluminum oxide and the refractory metals.

1.1.5. Theoretical Calculation Of Physical and Mechanical Properties

Calculations some properties of composite materials depend on the volume fraction of the matrix and the reinforcements. For this rule of the mixtures is used.

Density is calculated with this formula,

Consider two materials: reinforcing fibres with density ρ_f, matrix with density ρ_m, then the density of the composite material is given by

$$\rho_c = \rho_m V_m + \rho_f V_f \tag{1.1}$$

The other properties such as strength, stiffness can also be calculated in a similar manner.

1.1.6. Fabrication

An important aspect of composite materials concerns the technology by which they are produced. Depending on the nature of matrix and fibre and the required architecture of the fibre distribution, production at reasonable cost and with suitable microstructure quality can be a challenging problem.

Polymer Matrix Composites (PMC), there are many commercial processes for the manufacture of PMC components. These may be sub-divided in a variety of ways, but there are three main approaches to the manufacture of fibre-reinforced thermosetting resins and two distinct production methods for thermoplastic composites. A simple overview of

the starting materials and approaches adapted to their incorporation into components is given in Figure 1.3.

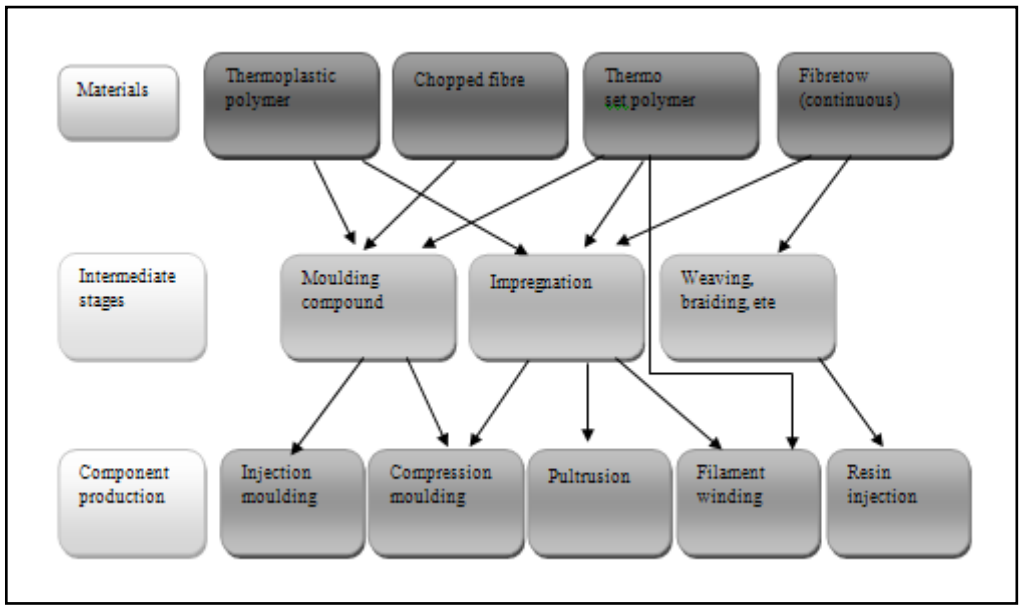

Figure 1.3. Schematic overview employed in fabrication of PMC [6]

Metal Matrix Composites (MMC), production of MMC is commercially less advanced than that of PMCs. Nevertheless, there has been considerable research effort into fabrication aspects, partly because the difficulties and cost of production have been largely responsible for their usage being relatively limited. The overview is presented in Figure 1.4

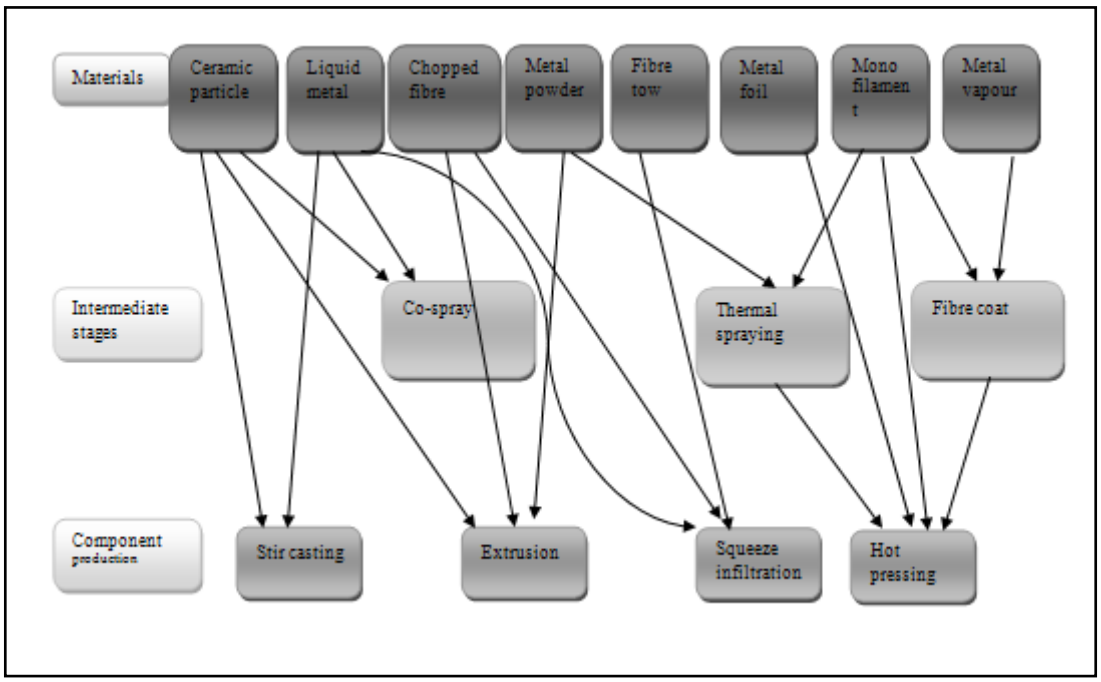

Figure 1.4. Schematic overview employed in fabrication of MMC [6]

1.1.7. Applications

Composite materials are used in a very wide range of industrial applications. A short summary is illustrated in Figure 1.5.

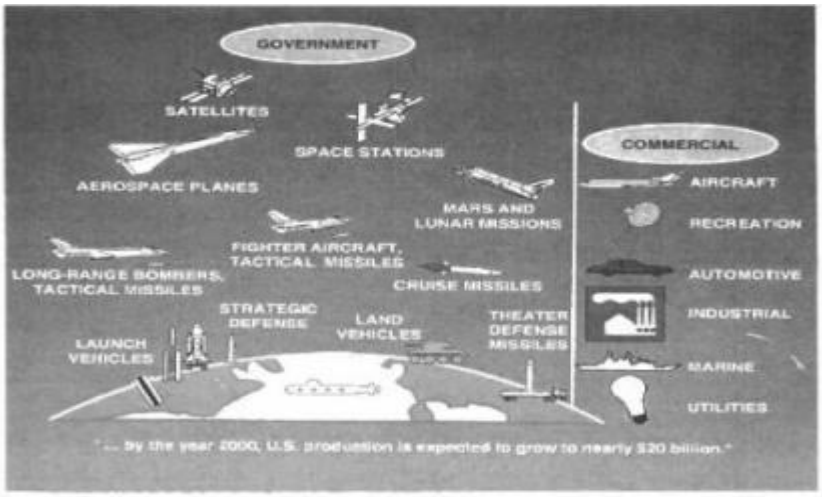

Figure 1.5. Composites usage area [7]

Minesweeper hull, glass-reinforced plastic is now very popular for various land and sea transport applications. While large ships are usually constructed from steel, over 80% of marine hulls less than about 40 m in length are made of glass-reinforcement plastic (Smith 1990). This is partly because fabrication in glass-reinforcement plastics more economic for relatively small craft.

Figure 1.6. Minesweeper hull [6]

Helicopter rotor blade good example of a component requiring excellent specific stiffness is helicopter rotor blades. Composites have been used for rotor blades since 1960s. Initial attractions of using composites included good fatigue resistance as well as specific stiffness.

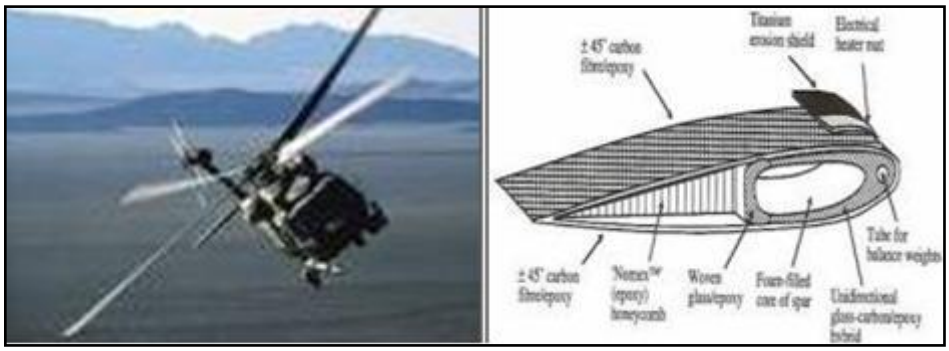

Figure 1.7. Schematic sections for a helicopter rotor blade [6]

There are many applications in sports goods with a requirement for stiff, slender beams. These include fishing rods, tennis racquets, skis surfboards and golf clubs. Polymer-based composites hold a dominant share in all such markets.

Figure 1.8. Golf driving club [6]

Al (6061) 10 % Al_2O_3 composite material is used in the mountain bikes and Al (2124) 20 % SiC is used in racing bikes. Both models have been successfully tested in extensive sports trials.

Figure 1.9. Bicycles [6]

Diesel engine piston, represents major early success in the industrial use of MMCs. Production in Japan has been increasing steadily over the past several years and now runs to millions of units annually. Originally, a Ni cast iron insert was used in the ring area of aluminum pistons.

Figure 1.10. Engine pistons [6]

Microelectronic devices often require stable environments. High-Ni steel or brazed steel molybdenum housings have been used to support ceramic (Al_2 O_3) substrate electronic packages.

Gas turbine combustor, can components at the hot end of a gas turbine are often exposed to very high temperatures and severe thermal shock conditions. The combustor can shown in Figure 1.11 provides a good example. A fuel /air mixture is fed through the first set of holes along the sides. The combustion temperatures along the periphery of the flame can reach 1500 ºC and the sides of the can rapidly become heated to temperatures close to this level (Schneider 1990). At such temperatures, most metals are molten, very soft, or, in the case of refractory metals such as molybdenum, prone to rapid oxidation. Some ceramic materials retain good strength and oxidation resistance under these conditions, but are likely to crack under the stresses generated by the high thermal gradients. The can shown in Fig 1.11 was fabricated from SiC layers approximately 200 μm thick, separated by thin ($\sim 7\mu m$), graphitic interlayers. The toughness and the resistance to thermal shock is raised considerably by the presence of the interfaces, at which any through-thickness cracks become deflected (Phillips 1993)

Figure 1.11. Gas turbine combustors can [6]

Aircraft brakes require a particularly demanding set of properties. During an emergency landing or aborted take-off, a very large amount of energy must be absorbed by the brakes in a short time without disintegration or seizure. Good thermal conductivity and high-temperature stability, solid graphite is a candidate material, which is much cheaper than carbon/carbon composite but the strength and toughness of the composite is superior[6].

Figure 1.12. Aircraft brake

Nanocomposites that consist of nanosized particles embedded in some type of matrix are a group of promising new materials. One type of nanocomposites is currently being used in high-performance tennis balls. These balls retain their original pressure and bounce twice as long as conventional ones. Schematic diagram of the cross-section of these tennis balls is shown in Figure 1.13.

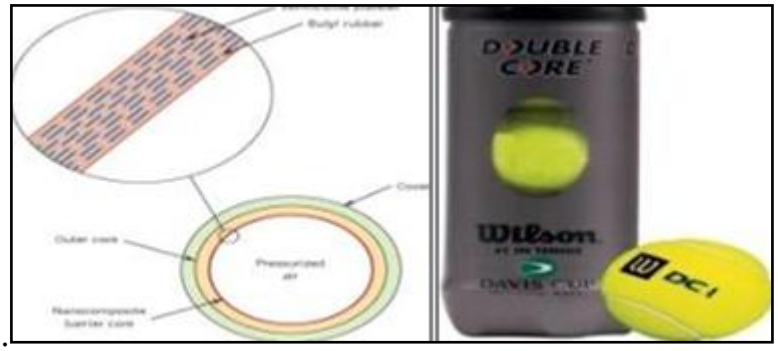

Figure 1.13. A nano composite tennis ball [4]

1.2. INTRODUCTION TO POWDER METALLURGY

A powder is defined as a finely divided solid, smaller than 1 mm in its maximum dimension. In most cases the powders will be metallic, although in many instances they are combined with other phases such as ceramics or polymers. An important characteristic of a powder is its relatively high surface area to volume ratio. The particles exhibit behavior that is intermediate between that of a solid and a liquid. Powders will flow under gravity to fill containers or die cavities, so in this sense they behave like liquids. They are compressible like a gas. However, the compression of a metal is essentially irreversible, like the plastic deformation of a metal. Thus, a metal powder is easily shaped with the desirable behavior of a solid after processing.

Powder metallurgy is the study of the processing of metal powders, including the fabrication, characterization and conversion of metal powders into useful engineering components [8].

1.2.1. Brief History

Ceramics, flour salt, sugar, minerals are powders. The uses of metal powders have been traced to several parts of the world. For example gold powder was fired onto jewelers by the Incas. Egyptian uses of iron powder date back to 3000 BC. Another example is the Delhi Column in India which dates from about 300 A. D. This column is made from 6.5

tons of reduced iron powder. The modern era of powder metallurgy is traced to Coolidge who used tungsten powder to develop a durable lamp filament for Edison [9].

1.2.2. Reasons For Using Powder Metallurgy

Many attributes contribute to the success of P/M. Three main categories contributing to the success of P/M. The intersection of the circles represents an ideal area for applying powder metallurgy in the future is shown in Figure 1.14.

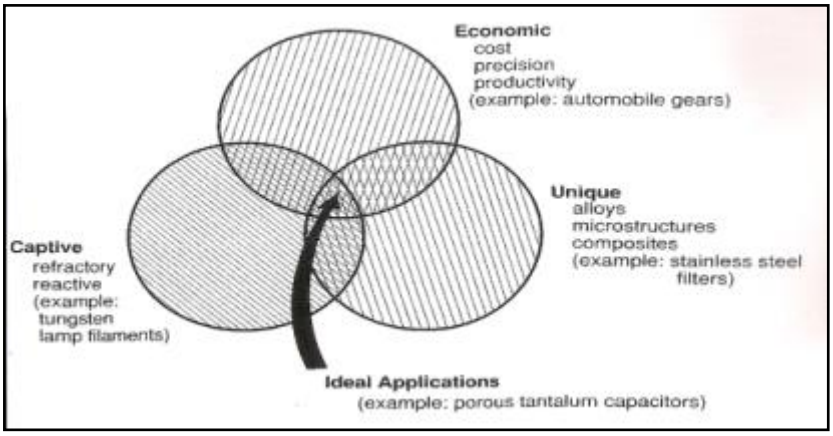

Figure 1.14. Powder metallurgy categorize [8]

The captive applications are those which are quite difficult to process by other techniques. Ideal examples are reactive and refractory metals for which melting is not practical.

The unique property examples include porous metals; oxide dispersion strengthened alloys, cermets (ceramic-metal composites) and cemented carbides. The inability to fabricate these unique microstructures by other techniques is another reason for using P/M.

Finally are the many applications which rely on the economical production of complex parts. Automotive industry presents good examples of this area.

1.2.3. Advantages And Disadvantages of P/M

P/M produced materials have disadvantages as well as advantages. Good understanding of these is essential in deciding matter of use P/M or not in a special application. The following table summarizes main advantages and disadvantages of P/M

Table 1.2. Advantages and disadvantages of P/M

Advantages	**Disadvantages**
Ability to create complex shapes	Cost of powder production
High strength properties	Limit on complexity of shapes
Low material waste	Size change during sintering
Good microstructure control	Potential work force health problems
Eliminates or minimizes machining	
Maintains close dimensional tolerances	
Properties and dimensions are easily controlled	
Wide variety of alloys	
Mass production	
Cost and energy efficient	

1.2.4. Physical Properties

Particle Size and measurement techniques; particle size is a nominal indicator of the dimensions of an average particle It depends on the measurement technique, parameter being measured and particle shape. Two of the most common measurement techniques are described below.

Microscopy method is widely applied technique for particle sizing uses ability of the eye to rapidly size dispersed particles in a microscope. Scanning Electron Microscopy is advantageous, since it shows surface topography and can provide x-rays for compositional analysis. By microscopic counting of diameter, length, height or area, a frequency

distribution can be generated. The distribution will record the relative frequency of the selected particle dimension.

The most commonly used method is screens of different mesh sizes. The most common convention for specifying mesh size relies on the number of wires per inch. Screen analysis begins with a stack of screens with decreasing mesh openings. As illustrated in Figure 1.15.

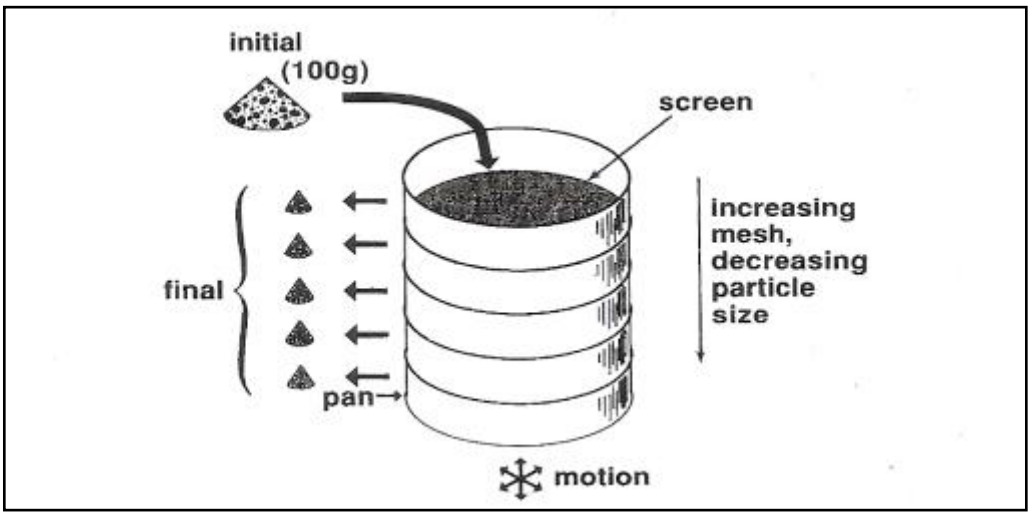

Figure 1.15. Screen analysis [8]

The other techniques are sedimentation light scattering, electrical zone sensing, light blocking, x-ray techniques comparison of particle size analysis approaches are shown in Table 1.3.

Table 1.3. Comparison of Particle Size Analysis Approaches

Technique	**Size range μm**	**Dynamic ratio**	**Sample size g**	**Relative speed***	**Basis+**
Microscopy					
Optical	0.8 and up	30	<1	S	P
Electron	0.001-400	30	<1	S	P
Sieving (wet and dry)					
Wire mesh	38 and up	20	100	I	W
Electroform	5-120	20	>5	S	W
Sedimentation					
Gravity	0.2-100	50	5	I	W
Centrifugal	0.02-10	50	1	S	W
Light scattering					
Fraunhofer	1-800	<200	<5	F	W
Mie	0.1-3	30	1	F	W
Velocity	0.5-200	400	1	F	P
Brownian	0-005-5	1000	<1	I	P
Electrical zone					
Sensing	0.4-1000	30	5	I	W
Light blocking	1-600	45	3	I	P
X-ray					
Broadening	0.01-0.2	-	1	S	P
Small angle	0.001-0.05	-	1	S	P
*S= slow (1 hour or more), I = intermediate (~1/2 hour),F= fast (1/4 hour or less) +P= population basis, W= weight basis					

Particle shape, influences packing, flow and compressibility and helps explain many processing characteristics. Figure 1.16. gives a collection of particle shapes. Particle shape changes with size and manufacturing technique. Gas or air atomization produces more

rounded particles irregular shapes are produced water atomization technique. Irregular particle shape can also be expressed by the ratio is the diameter of the outer circle to equivalent spherical diameter. Control of particle shape achieved by optical and electron microcopies.

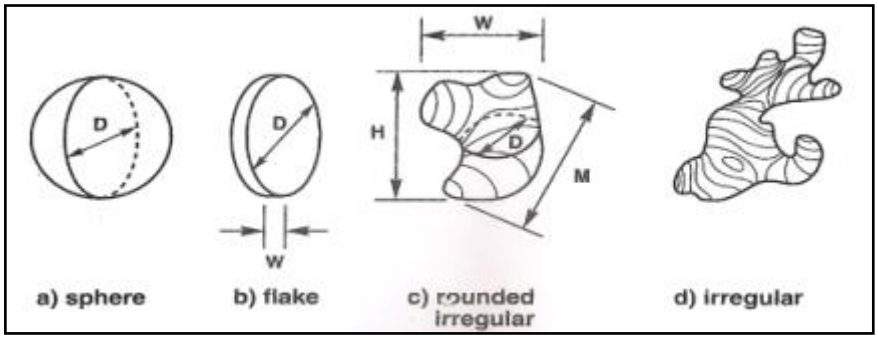

Figure 1.16. Some particle shapes

Compressibility one of the main uses for metal powders is for fabricating complex shapes by compaction. Compressibility or compactability measures the ability to density a powder under an applied load. The die is loaded with powder and the density is measured after compaction at a predetermined pressure, often near 414 MPa. This is termed the green density and is the basis for expressing the compressibility. A parameter used in tool design is the compression ratio C_R ,

$$C_R = \frac{V_L}{V_C} = \frac{\rho_g}{\rho_a} \tag{1.2}$$

ρ_g is green density

ρ_a is apparent density

V_L is Volume of the loose powder

V_C is Volume of the compacted powder

Sintering; sintering is the bonding together of particles at high temperatures below melting point by solid-state atomic transport events, but in many instances involves the formation of a liquid phase. Particles sinter by atomic motions that eliminate the high surface energy associated with powder. The surface energy per unit volume depends on the inverse of the particle diameter. Smaller particles with high specific surface areas have more energy and sinter faster.

Consider two spherical particles in contact. In powder compacts there are many such contacts on each particle. The bonds between contacting particles enlarge and merge as sintering progresses. At each contact a particle boundary grows to replace the solid-vapor interface.

The two sphere sintering model with the development of the interparticle bond during sintering starting with a point contact. Neck growth creates a new particle boundary at the particle contact and if time is sufficient the two particles with eventually coalesce into a single large particle and the final diameter equal to 1.26 times the original diameter [8].

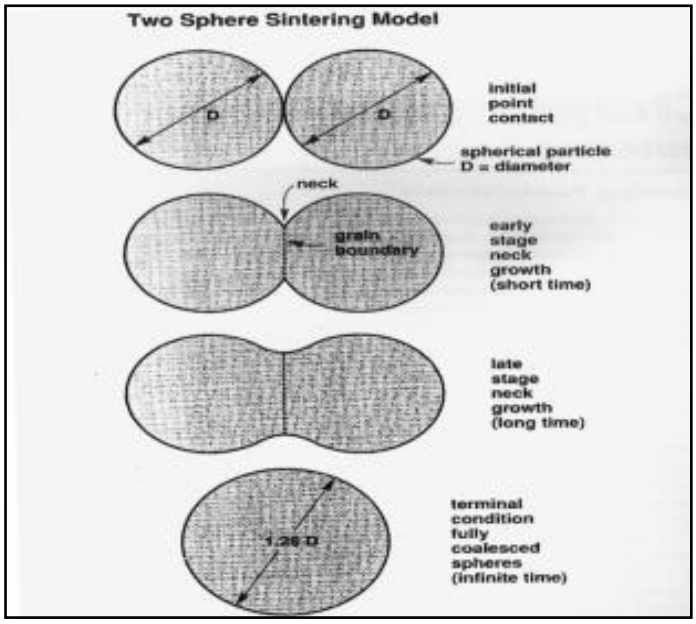

Figure 1.17. Two sphere sintering models [8]

Table 1.4. Sintering temperature and time for various metals [10]

Material	**Temperature ºC**	**Time (Min)**
Copper, brass and bronze	760-900	10-45
Iron and iron-graphite	1000-1150	8-45
Nickel	1000-1150	30-45
Stainless steels	1100-1290	30-60
Alnico alloys	1200-1300	120-150
Ferrites	1200-1500	10-600
Tungsten carbide	1430-1500	20-30
Molybdenum	2050	120
Tungsten	2350	480
Tantalum	2400	480

1.2.5. Applications

Many P/M parts now used in a variety of industries, including automobiles, household appliances, yard and garden equipment and orthodontic devices, etc; Some applications showed in Table 1.5.

Table 1.5. Example Applications for Metal Powders [8]

Applications	**Example Uses**
Agriculture	seed coatings, lawn and garden equipment
Abrasives	metal polishing wheels, grinding media
Aerospace	jet engines, heat shields, rocket nozzles
Automotive	valve inserts, bushings, gears, connecting rods
Chemicals	colorants, filters, catalysts
Coatings	paint, hard facings, thermal spray barriers
Construction	asphalt, roofing, caulking
Electrical	contacts, wire clamps, brazes, connectors
Electronic	heat sinks, inks, microelectronic packages
Hardware	locks, wrenches, cutting tools
heat treating	furnaces, thermocouples, conveyor trays
Industrial	sound adsorption, cutting tools, diamond bonds
Joining	solders, electrodes, weld filler
Lubrication	greases, abatable seals
Magnetic	relays, magnets, cores
Manufacturing	dies, tools, bearings, hard facing
medical/dental	hip implants, amalgams, forceps
Metallurgical	metal recovery, alloying
Nuclear	shielding, filters, reflectors
Office equipment	copiers, cams, gears, photocopy process carrier
Ordnance	fuses, ammunition, penetrators
Personnel	vitamins, cosmetics, soaps, ballpoint pens
Petrochemical	catalysts, drilling bits
Plastics	tools, dies, fillers, cements, wear surfaces
Printing	inks, coatings, laminates
Pyrotechnics	explosives, flares, fuel, colorants

1.3. PRODUCTION OF ALUMINUM POWDER

Aluminum powders are produced by gas atomization. The used gas is compressed air. In some special cases inert gases are used. Atomized aluminum powders are used in a variety of applications that include explosives, rocket fuel, chemical processes, pharmaceuticals, and pigments for paints and printing inks. In recent years automotive applications are increased [11].

1.3.1. General Atomizing Process For Aluminum

There are many methods to produce aluminum and aluminum alloy powders including gas and centrifugal atomization ultrasonic or pulsed atomization. Gas atomization's is used for several applications. Atomized aluminum powder grades are produced by atomizing molten aluminum [11-12].

The molten aluminum is drawn through an atomizing nozzle. The lower end of the nozzle dips into the molten aluminum and the upper end terminates in a small chamber into which a jet of pressurized air or inert gas is introduced. The air jet impinges on the stream of molten aluminum and disintegrates it into small particles [13].

Then particles drawn through a chiller chamber into the collection system consisting of two sets of cyclones. After the cyclones the powder is transported in an atmosphere of inert gas to the screens and packed [11].

1.3.2. Powder Size And Shape Of Aluminum

The electron micrograph in Figure 1.18. shows spherical, and irregular, nodular shape of conventional air-atomized aluminum powders. In most aluminum powder manufacturing methods, compressed air is used as the atomizing medium. Inert gases are used only for specialty applications that require a specific particle shape [13].

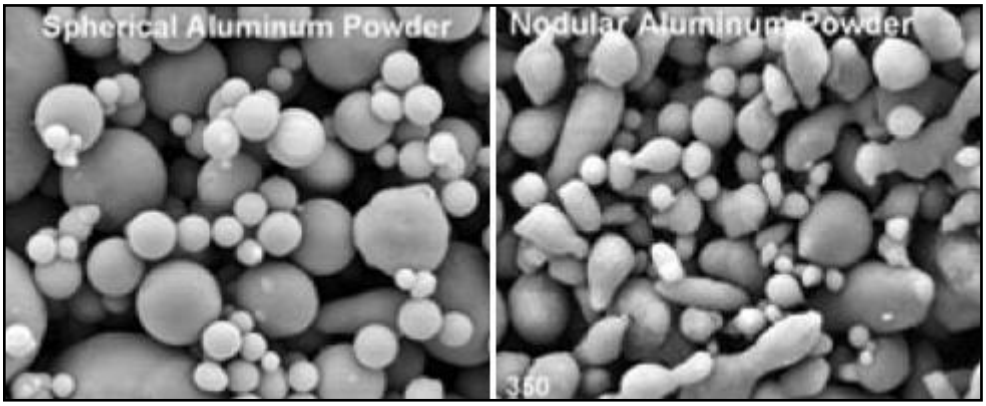

Figure 1.18. Some examples of Aluminum Powders [14]

Figure 1.19. shows particle size distribution curves for typical coarse medium and fine grades of atomized powders.

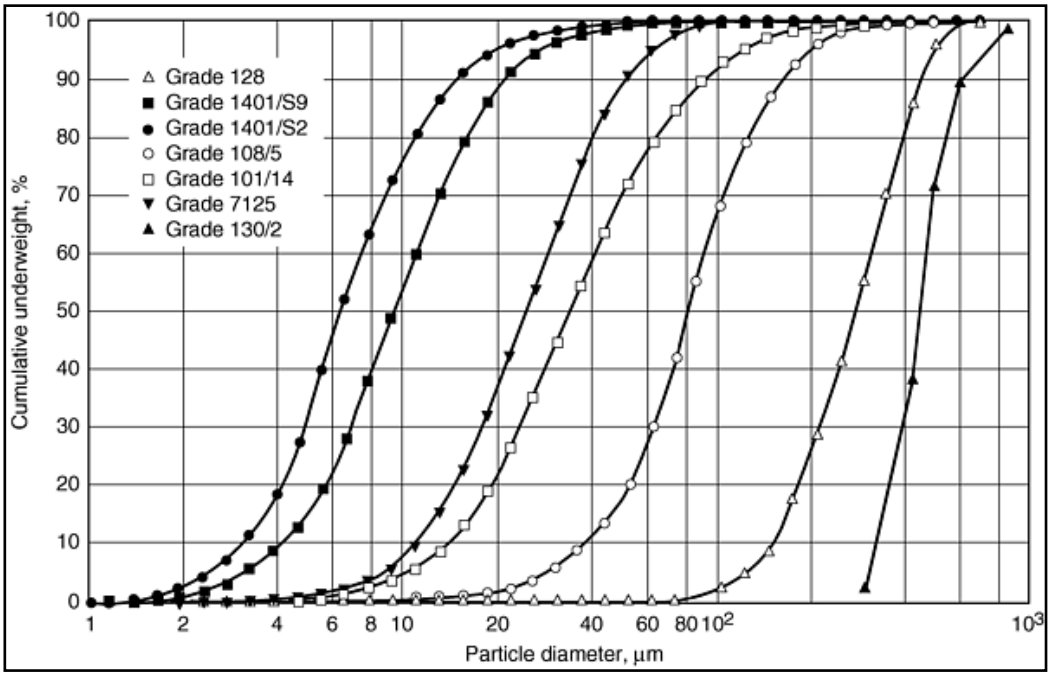

Figure 1.19. Particle size distributions in some Alcoa powder grades [11-14]

Gas sorption methods are employed for measurements of total surface area .The specific surface area of aluminum powders is determined by the size distribution and the morphology of the particle powders atomized in air show a larger area than inert gas

atomized powders due to the irregular shape. The surface area of various atomized aluminum powders are shown in Table 1.6. and Figure 1.20.

Table 1.6. The surface areas of various atomized aluminum powders [15]

Aluminum	**Gas-sorption area m^2/g**
Coarse(40 mesh designation)	0.15
Fine	0.25
Dust collector-fine (325 mesh designation)	0.90

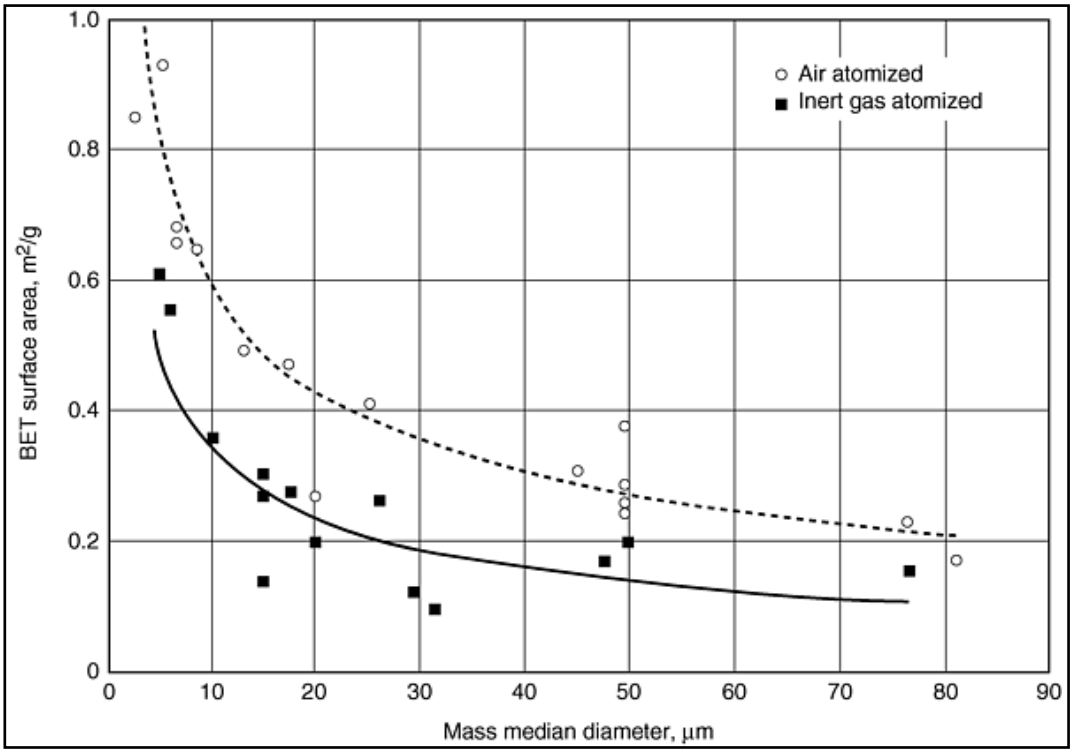

Figure 1.20. Surface area for aluminum powders atomized in air and in inert gas [11]

1.3.3. Physical Properties

Typical physical properties of atomized aluminum powders are shown in Table 1.7.

The real density of aluminum powder approaches that the base metal, but both apparent density and tap density vary as a function of particle size distribution [11].

Table 1.7. Physical properties of atomized aluminum powders [16-17]

Wrought density	2.7 g/cm³
Melting point	660 ºC
Boiling point	2430ºC
Surface tension at 800ºC	865 dynes/cm
Apparent density	0.8 to 1.3 g/cm³
Tap density	1.2 to 1.5 g/cm³
Melting point of oxide	2045ºC
Al_2O_3 content	0.1 to 1.0 wt%

1.3.4. Chemical Properties

The chemical compositions of unalloyed atomized aluminum powders are shown in Table 1.8. Iron and silicon are the major contaminants for both regular and high-purity powders. Aluminum is stable in air because of its thin, natural oxide film, however aluminum is more chemically reactive and hydrates when exposed to moisture. Powders also react with water [11].

Table 1.8. Typical chemical analyses of atomized aluminum powders [13]

Type of powder	**composition, wt %**			**other metallic**	
	aluminum	**iron**	**silicon**	**each**	**total**
Atomized powders					
Typical	99.7				
Maximum		0.25	0.15	0.05	0.15
High-purityatomized powders					
Minimum	99.97				
Typical	99.976	0.007	0.008		0.009

1.3.5. Aluminum P/M Parts Processing

Aluminum P/M parts are compacted at low pressures and are adaptable to all types of compacting equipment. Figure 1.21 shows the relative difference in compacting characteristics for aluminum and sponge iron or copper.

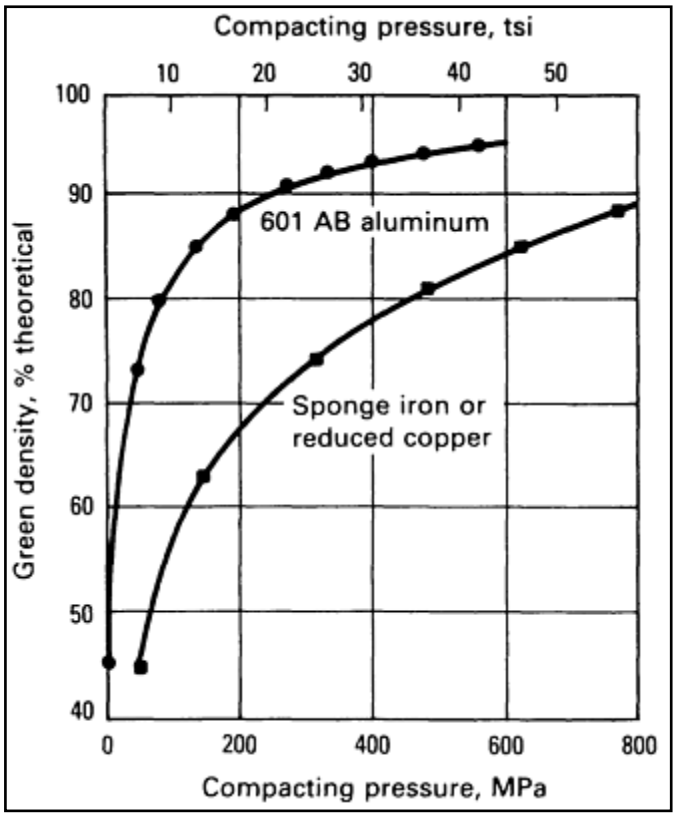

Figure 1.21. Relationship of green density and compacting pressure [13]

The lower compacting pressures required for aluminum. Depending on the press a larger part often can be made by taking advantage of maximum press force. In addition aluminum responds better to compacting and moves more readily in the die more complex shapes having more precise and finer detail can be produced.

Aluminum P/M parts can be sintered in a controlled, inert atmosphere or in vacuum. Sintering temperatures are based on alloy composition and generally range from 595 to 625 ºC (1100 to 1160ºF). Sintering time varies from 10 to 30 min. Nitrogen, dissociated ammonia, hydrogen; argon and vacuum have been used for sintering aluminum.

Table 1.9. Typical properties of nitrogen-sintered Al. P/M alloys [13]

Alloy	Compacting pressure		Green density		Green strength		Sintered density		Temper	Tensile strength		Yield strength		Elongation%	Hardness
	Mpa	tsi	%	g/cm³	Mpa	psi	%	g/cm³		Mpa	ksi	Mpa	ksi		
601AB	96	7	85	2,29	3,1	450	91,1	2,45	T1	110	16	48	7	6	55-60 HRH
									T4	141	20,5	96	14	5	80-85 HRH
									T6	183	26,5	176	25,5	1	70-75 HRE
	165	12	90	2,42	6,55	950	93,7	2,52	T1	139	20,1	88	12,7	5	60-65 HRH
									T4	172	24,9	114	16,6	5	80-85 HRH
									T6	232	33,6	224	32,5	2	75-80 HRE
	345	25	95	2,55	10,4	1500	96	2,58	T1	145	21	94	13,7	6	65-70 HRH
									T4	176	25,6	117	17	6	85-90 HRH
									T6	238	34,5	230	33,4	2	80-85 HRE
602AB	165	12	90	2,42	6,55	950	93	2,55	T1	121	17,5	59	8,5	9	55-60 HRH
									T4	121	17,5	62	9	7	65-70 HRH
									T6	179	26	169	24,5	2	55-60 HRE
	345	25	95	2,55	10,4	1500	96	2,58	T1	131	19	62	9	9	55-60 HRH
									T4	134	19,5	65	9,5	10	70-75 HRH
									T6	186	27	172	25	3	65-70 HRE
201AB	110	8	85	2,36	4,2	600	91	2,53	T1	169	24,5	145	24	2	60-65 HRE
									T4	210	30,5	179	26	3	70-75 HRE
									T6	248	36	248	36	0	80-85 HRE
	180	13	90	2,5	8,3	1200	92,9	2,58	T1	201	29,2	170	24,6	3	70-75 HRE
									T4	245	35,6	205	29,8	4	75-80 HRE
									T6	323	46,8	322	46,7	1	85-90 HRE
	413	30	95	2,64	13,8	2000	97	2,7	T1	209	30,3	181	26,2	3	70-75 HRE
									T4	262	38	214	31	5	80-85 HRE
									T6	332	48,1	327	47,5	2	90-95 HRE

Aluminum can be sintered in batch furnaces or continuous radiant tube mesh furnaces, or cast belt furnaces. Optimum dimensional control is best attained by maintaining furnace temperature at $\pm$ 2.8 ºC.

Mechanical properties are directly affected by thermal treatment. All compositions respond to solution heat treating, quenching and aging in the same manner as conventional heat-treatable alloys [13].

1.3.6. Properties of Sintered Parts

The benefits of using P/M techniques for lightweight metal applications are exemplified by aluminum. In using aluminum P/M parts for special applications, a variety of improved material characteristics are available

Weight Reduction; aluminum enjoys a considerable weight advantage over competing P/M materials, assuming strength requirements are not high.

Aluminum P/M parts weigh one-third as much as the same parts made from iron or copper powders. Lightweight aluminum parts reduce power requirements in drive motors and minimize vibration and noise in machinery that has unbalanced rotary or reciprocating motions. Aluminum P/M components are lower in cost than titanium or beryllium P/M components.

Corrosion resistance aluminum P/M parts are used extensively in both structural and nonstructural applications because of corrosion resistance properties. Corrosion resistance can be further improved by the application of chemical conversion coatings or anodizing treatments.

Mechanical Properties; sintered aluminum P/M parts can be produced with strength that equals or exceeds that of iron or copper P/M parts. Tensile strengths range from 110 to 345MPa depending on composition, density sintering practice, heat treatment and re-pressing procedures.

Table 1.10. list typical properties of four nitrogen-sintered P/M alloys. Properties of heat-threaded pressed and sintered aluminum P/M alloys. Properties of heat –treated, pressed and sintered grades are provided in Tables 1.11.

Table 1.10. Typical heat-treated properties of nitrogen-sintered al. P/M alloys [13]

Heat-treated variables and properties	**Grades**			
Solution treatment	**MD-22**	**MD-24**	**MD-69**	**MD-76**
Temperature, °C (°F)	520 (970)	500 (930)	520 (970)	475 (890)
Time,min	30	60	30	60
Atmosphere	Air	Air	Air	Air
Quench medium	H_2O	H_2O	H_2O	H_2O
Aging				
Temperature, °C (°F)	150 (300)	150 (300)	150 (300)	125 (257)
Time,h	18	18	18	18
Atmosphere	Air	Air	Air	Air
Heat-treated (T_6) properties(a)				
Transverse-rupture strength, Mpa (ksi)	550 (80)	495 (72)	435 (63)	435 (63)
Yield strength,Mpa (ksi)	200 (29)	195 (28)	195 (28)	275 (40)
Tensile strength, Mpa (ksi)	260 (38)	240 (35)	205 (30)	310 (45)
Elongation. %	3	3	2	2
Rockwell hardness, HRE	74	72	71	80
Electrical conductivity, %IACS	36	32	39	25

Table 1.11. Room-temperature of pressed and sintered aluminum alloy test bars [13]

Alloy designation	**Nominal composition**	**Temper designation**	**Density, % of theoretical**	**Tensile strength**		**Yield strength**		**Elogation in 25 mm (1 in), %**
				Mpa	**ksi**	**Mpa**	**ksi**	
601AB	1.0 Mg 0.6 Si,	T1	91.1	110	16	48	7	6
	0.25 Cu, rem Al	T4	91.1	141	20,5	97	14	5
		T6	91.1	183	26,5	176	25,5	1
		T61	…	241	35	237	34,4	2
		T1	93.7	121	17,5	55	8	7
		T4	93.7	148	21,5	100	14,5	5
		T6	93.7	224	32,5	214	31	2
		T61	…	252	36,5	247	35,8	2
		T1	96.0	124	18	59	8,5	8
		T4	96.0	152	22	103	15	5
		T6	96.0	252	36,5	241	35	2
		T61	…	255	37	248	36,2	2
201AB	0.5 Mg, 0.8 Si,	T1	91.0	169	24,5	145	21	2
	4.4 Cu,rem Al	T4	91.0	210	30,5	179	26	3
		T6	91.0	248	36	…	…	…
		T61	…	343	49,7	339	49,2	0,5
		T1	92.9	201	29,2	170	24,6	3
		T4	92.9	245	35,6	205	29,8	3,5
		T6	92.9	322	46,8	…	…	…
		T61	…	349	50,6	342	49,6	0,5
		T1	97.0	209	30,3	181	26,2	3
		T4	97.0	262	38	214	31	5
		T6	97.0	332	48,1	327	47,5	2
		T61	…	356	51,7	354	51,3	2

1.3.7. Fields of Application

Aluminum P/M parts are used in an increasing number of applications. The business machine market currently uses the greatest variety of aluminum P/M parts. Other markets that indicate growth potential include automotive components, aerospace components, power tools, appliances, and structural parts. Power tools, appliances and structural parts

Figure 1.22. Machining chips from a P/M aluminum alloy[13]

Materials substitution is a key concern in the automotive industry. The desire to use lightweight corrosion resistant materials should promote increased interest in aluminum P/M parts. an aluminum P/M shock absorber piston that offers 15% more strength than competing iron P/M parts.

Other applications; aluminum P/M parts also are being used for applications figure1.23 shows typical parts. The light-weight aluminum parts reduce noise and vibration during operation. The thermal conductivity of aluminum makes it an ideal material for heat sinks [11].

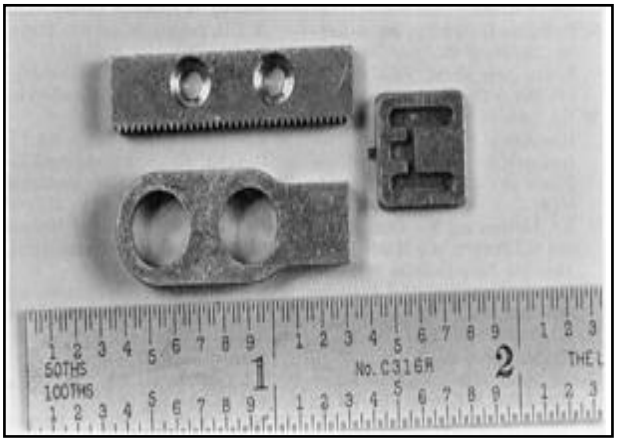

Figure 1.23. Aluminum P/M parts

1.4. ALUMINUM BORON CARBIDE

1.4.1. Boron

Boron was discovered by the french chemists Joseph Gay-Lussac and Louis Thenard and by the british chemist Sir Humphry Davy. Boraks, the most widely used type known for thousands of years.

All the elements are classified in the periodic table according to electron configuration

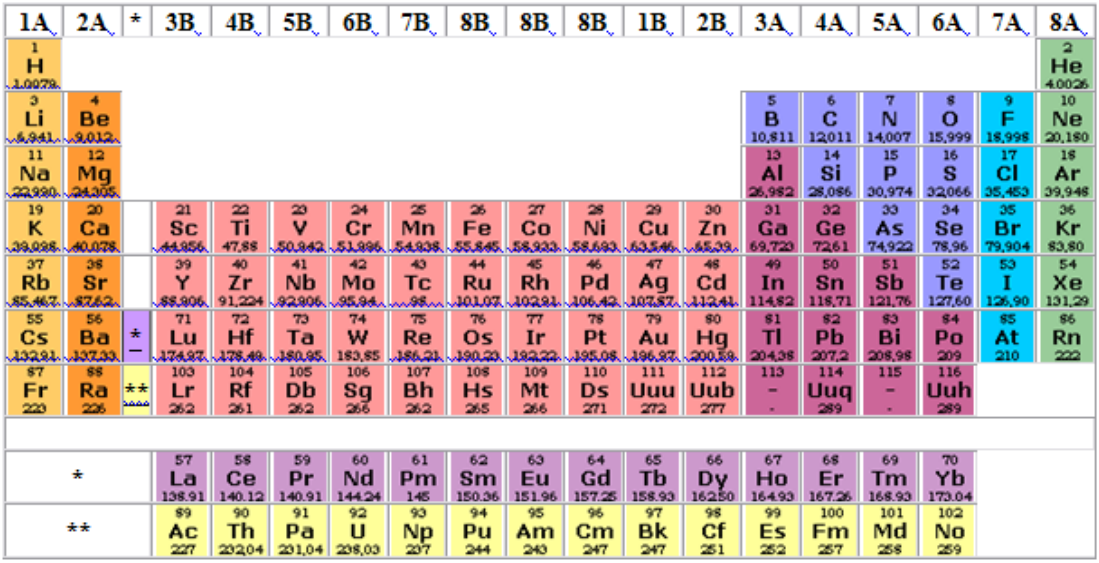

Figure 1.24. Periodic table

Boron is positioned in the group 3A and displays characteristic that are intermediate between the metals and nonmetals Atomic number is 5, atomic weight is 10.811, melting point is 2348 ^{0}K boiling point is 4273 ^{0}K

It does not occur as free element in nature. Usually, it occurs as a mineral with associated clay and other impurities. These ores can be refined into pure chemical compounds of commercial importance.

Some compounds are:

Boric acid	H_3BO_3
Anhydrous boric acid	B_2O_3
Anhydrous borax	$Na_2B_4O_7$
Borax pentahydrate	$Na_2B_4O_7.10H_2O$
Borax decahydrate	$Na_2B_4O_7.5H_2O$
Sodium Perborate	$Na_2B_4O_7.\ 5H_2O$

Some commercially important boron minerals are,

Tincal	$Na_2B_4O_710H_2O$
Kernite	$Na_2B_4O_7\ 4H_2O$
Colenanite	$Ca_2B_6O_{11}\ 5H_2O$
Ulexite	$NaCaB_5O_98H_2O$
Datolit	$Ca_2B_2O_5Si_2O_5H_2O$
Hydroboracite	$CaMgB_6O_{11}6H_2O$

The important factor for industrial application of boron minerals are B_2O_3 content. Boron minerals contain different amount of B_2O_3 in their structures. Turkey is the largest producer of boron ore in the world as shown in Table 1.12.

Table 1.12. World Boron Reserves (Thousand Tons - B_2O_3)

Country	**Proven Reserve**	**Probable Possible Reserve**	**Total Reserve**	**Percent in Total (%)**
Turkey	227.000	624.000	851.000	72.20
U.S.A.	40.000	40.000	80.000	6.80
Russia	40.000	60.000	100.000	8.50
China	27.000	9.000	36.000	3.10
Chile	8.000	33.000	41.000	3.50
Bolivia	4.000	15.000	19.000	1.60
Peru	4.000	18.000	22.000	1.90
Argentina	2.000	7.000	9.000	0.80
Kazakhstan	14.000	1.000	15.000	1.30
Serbia	3	0	3	0.30
Total	369.000	807.000	1,176.000	100

1.4.2. Boron in Use

- Boron minerals have a very wide range of applications
- Agriculture
- Detergents
- Ceramic
- Glass
- Timber Preservation (prevents and controls the spread of bacteria)
- Flame Retardants
- Nuclear Power Stations
- Cosmetics and medicine
- Metallurgy
- Glass
- Magnets
- Automobile airbags

- Photography
- Fuels
- Vehicle plates and gun barrels

1.4.3. Boron Carbide

Boron Carbide whose chemical formula is B_4C is extremely hard ceramic material. It is one of the hardest materials known after cubic boron nitride and diamond. Properties of B_4C are molar mass 55, 255 g/mol; appearance is dark grey on black powder,density is 2.52 g/cm^3, solid melting point is 2350^{o}C, boiling point is 3500^{o}C and crystal structure is rhombohedra.

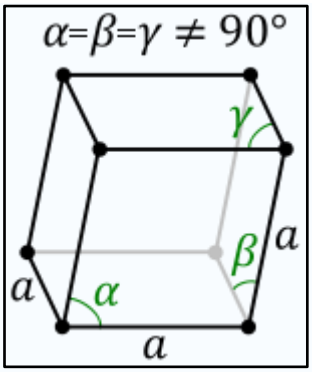

Figure 1.25. Crystal structure

Boron carbide is produced in electrical arc furnace by the reduction method from

B_2O_3 as boron oxide or H_3BO_3 as boron acid

$2B_2O_3 + 7C \rightarrow B_4C + 6CO_2$

or

$4H_3BO_3 + 7C \rightarrow B_4C + 6CO + 6H_2O$

Table 1.13. Fepa Standard of Boron Carbide particle size distribution

B Particle size	Coarsest Size			Coarser Size			Basic Size			Mixed Size				Coarse Size		
	Sieve Size		Residue on sieve	Sieve Size		Residue on sieve	Sieve Size		Residue on sieve	Sieve Size			Residue on sieve	Sieve Size		Residue under sieve
	mm	µm	Mess fraction %	mm	µm	Mess fraction %	Mm	µm	Mess fraction %	Mm		µm	Mess fraction %	mm	µm	Mess fraction %
F4	8.00	-	0	5.60	-	20	4.75	-	40	4.75	4.00	-	70	3.35	-	3
F5	6.70	-	0	4.75	-	20	4.00	-	40	4.00	3.35	-	70	2.80	-	3
F6	5.60	-	0	4.00	-	20	3.35	-	40	3.35	2.80	-	70	2.36	-	3
F7	4.75	-	0	3.35	-	20	2.80	-	40	2.80	2.36	-	70	2.00	-	3
F8	4.00	-	0	2.80	-	20	2.36	-	45	2.36	2.00	-	70	1.70	-	3
F10	3.35	-	0	2.36	-	20	2.00	-	45	2.00	1.70	-	70	1.40	-	3
F12	2.80	-	0	2.00	-	20	1.70	-	45	1.70	1.40	-	70	1.18	-	3
F14	2.36	-	0	1.70	-	20	1.40	-	45	1.40	1.18	-	70	1.00	-	3
F16	2.00	-	0	1.40	-	20	1.18	-	45	1.18	1.00	-	70	-	850	3
F20	1.70	-	0	1.18	-	20	1.00	-	45	1.00			850	70	-	710
F22	1.40	-	0	1.00	-	20	-	850	45	-	850	710	70	-	600	3
F24	1.18	-	0	-	850	25	-	710	45	-	710	600	65	-	500	3
F30	1.00	-	0	-	710	25	-	600	45	-	600	500	65	-	425	3
F36	-	850	0	-	600	25	-	500	45	-	500	425	65	-	355	3
F40	-	710	0	-	500	30	-	425	40	-	425	355	65	-	300	3
F46	-	600	0	-	425	30	-	355	40	-	355	300	65	-	250	3
F54	-	500	0	-	355	30	-	300	40	-	300	250	65	-	212	3
F60	-	425	0	-	300	30	-	250	40	-	250	212	65	-	180	3
F70	-	355	0	-	250	25	-	212	40	-	212	180	65	-	150	3
F80	-	300	0	-	212	25	-	180	40	-	180	150	65	-	125	3
F90	-	250	0	-	180	20	-	150	40	-	150	125	65	-	106	3
F100	-	212	0	-	150	20	-	125	40	-	125	106	65	-	75	3
F120	-	180	0	-	125	20	-	106	40	-	106	90	65	-	63	3
F150	-	150	0	-	106	15	-	75	40	-	75	63	65	-	45	3
F180	-	125	0	-	90	15	-	63	40	-	63	53	65	-	-	-
F220	-	106	0	-	75	15	-	53	40	-	53	45	60	-	-	-

Table 1.14. Fepa Standard of Boron Carbide particle size distribution continue

Particle Size	**D3**	**D50**	**D95**
F230	77 Max.	55. 7±3. 0	38 min.
F240	68 Max.	47. 5±2. 0	32 min.
F280	60 Max.	39. 9±1. 5	25 min.
F320	52 Max.	32. 8±1. 5	19 min.
F360	46 Max.	26. 7±1. 5	14 min.
F400	39 Max.	21. 4±1. 0	10 min.
F500	34 Max.	17. 1±1. 0	7 min.
F600	30 Max.	13. 7±1. 0	4. 6 min.
F800	28 Max.	11. 0±1. 0	3. 5 min.
F1000	23 Max.	9. 1±0. 8	2. 4 min.
F1200	20 Max.	7. 6±0. 5	2. 4 min.

Table 1.15. Content of Aluminum

Al	**Fe**	**Si**	**Cu**	**Zn**	**Ti**	**Mn**	**Others**	
							Amount	**Total**
99. 50	0. 25	0. 15	0. 03	0. 04	0. 03	-	0. 03	0. 10

Aluminum powder size was 63-100 μm, particle shapes were irregular and fabrication method was atomization.

2. LITERATURE SURVEY

Mohanty and friends studied boron carbide reinforced aluminum 1100 matrix composites, fabrication and properties. Aluminum 1100 size 30-45 μm purity was 99,9% was mixed with B_4C composition from 0-6-10-15 and 25 wt % in a ball mill at 120 rpm 300 min. Samples size was 50 mm -13 mm -3,2 to 5,9 mm were prepared by uniaxial pressing in a rectangular die at 90 MPa. All the samples were vacuum sintered at 873 ºK for 90 min by gas quenching to room temperature.

Density, electrical conductivity, hardness tests were examined. Density measured by Archimedes method. Vickers micro hardness measured. For fractography SEM (scanning electron microscopy) was used.

AlB_2 and Al_3BC phases were developed at temperature greater than 1173 ºK [18].

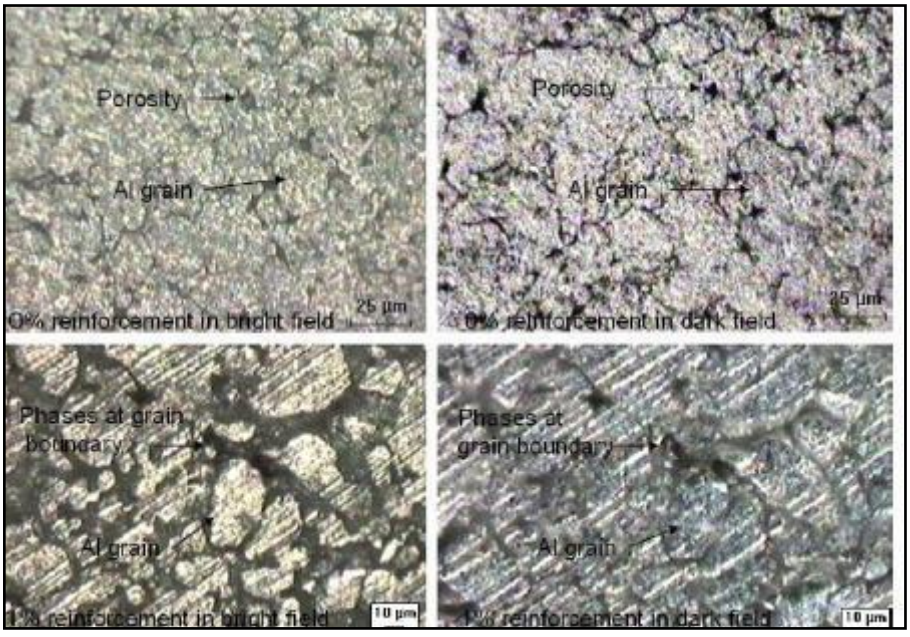

Figure 2.1. Microstructure of 0% and 1% B_4C-Al 1100 by XRD [18]

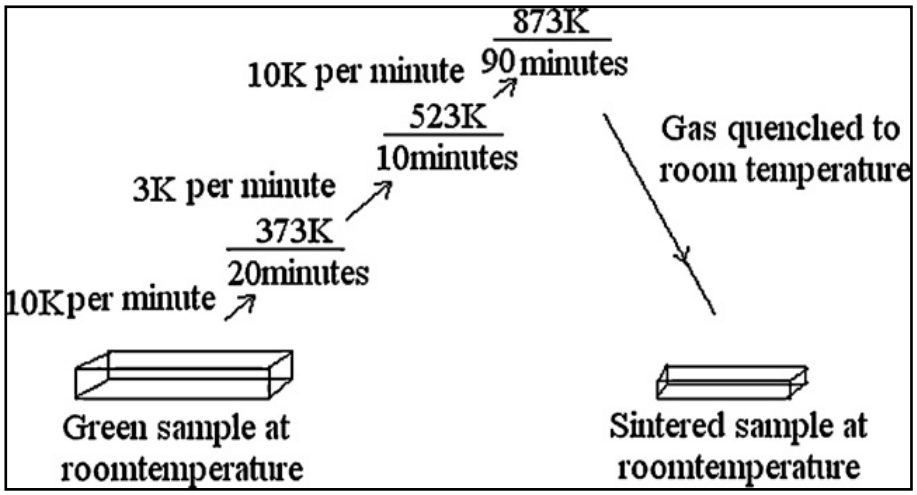

Figure 2.2. Heat treatment schedule as followed for sintering the MMCs [18]

Results; with increased percentage of B_4C reinforced material increased the porosity. The electrical conductivity decreased with increasing percentage B_4C.Hardness for up to 6 wt% of B_4C was increase in hardness was linear between 10 wt% and 25wt% reinforcement the increase was sharp. Flexure and deflection versus boron carbide percentage were decreased. Microstructure phases are presented in Figure 2.1.

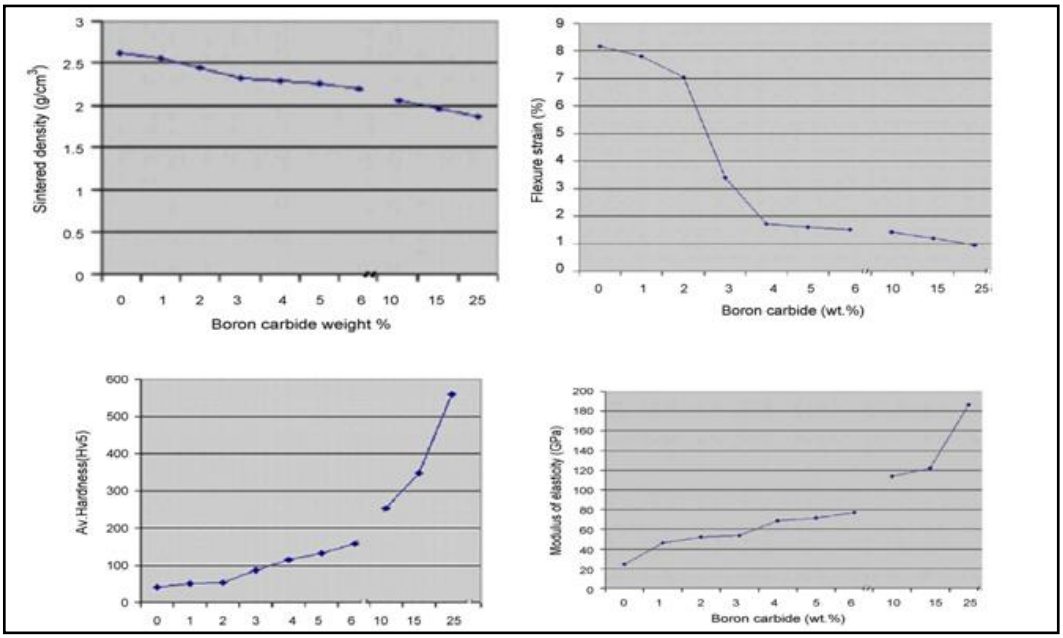

Figure 2.3. Density, strain, hardness, modulus of elasticity

The hardness improved with increase of reinforcement from 0 wt% to 25 wt%, Modulus of elasticity rise from 22GPa to 185 GPa at 25wt% reinforcement. Density decreased from 2.52 g/cm^3 to 1.8 g/cm^3[18].

Topcu and friends studied B_4C reinforced Al matrix composites processing and mechanical properties.

They used 5-10-15-20 wt% B_4C particles of 10 μm size Al powders 99,99% purity, density, 2,699 g/cm^3 with a 10 μm size were used as raw material. The ball to powder weight ratio was 6:1 milling speed was 400 rpm ball diameter 10mm. Powder materials were pressed at 250 MPa sintering atmosphere was argon and sintering of specimens were carried out at 3 different temperatures 600-625-640 ºC Microstructures investigated by SEM equipment, X-Ray diffractometer analysis performed. Hardness, and densities measured. The lengths of the composites had 12mm diameter 24-40mm in length creep behavior of the materials was investigated. The theoretical densities of specimens have been calculated as follow formula;

$$\frac{1}{\rho_c} = \frac{w_t}{\rho_t} + \frac{w_m}{\rho_m} \tag{2.1}$$

The density increased according to sintering temperature for all different B_4C contents. However low B_4C content had closer results. In density B_4C particles are distributed homogenously in the matrix. X-Ray diffractions of the samples at various B_4C

Content shows the peaks at 2θ of 38,44º and 44,7º belongs to the pure Al and 37,8º and 23,49º belongs to the B_4C.

The Vickers hardness tests performed increased weight percent of B_4C and sintering temperature increased the hardness of the composite.

Impact test results was the increase in B_4C content reduction in impact résistance. Creep test were investigated. Specimens with a gauge diameter of 12-15mm and length of 25-30mm were machined from the CIP rods. Specimens sintered at 650 ºC for 1h.Creep

tests were conducted at 400 and 450ºC.Temperature of the specimens was monitored by three separated thermocouples. The creep tests lasted for 6h.It is clear that creep strain was decreased with increasing B_4C content [3].

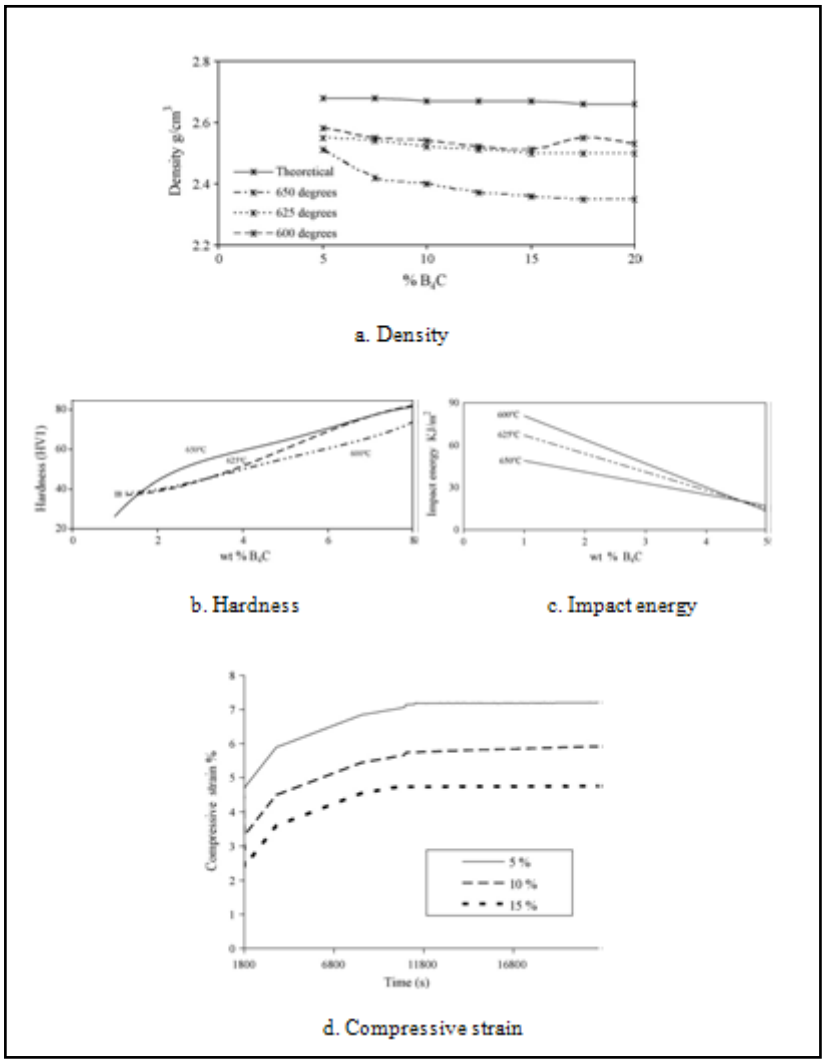

Figure 2.4. (a) density, (b) hardness, (c) impact energy, (d) compressive strain [3]

Mashhadi and friends studied the effect of Al addition on pressureless sintering of B_4C ceramic. Different amount of Al, from 0 to 5 wt% were added to the base material and pressureless sintering was conducted at 2050ºC and 2150ºC under argon atmosphere. Microstructure, crystal phases and density evolution were studied and correlated to Al additions. Density and particle size of sintered samples increased, porosity decreases significantly with aluminum.

Adding Al and increasing the sintering temperature increases shrinkage of the sintered B_4C samples [19].

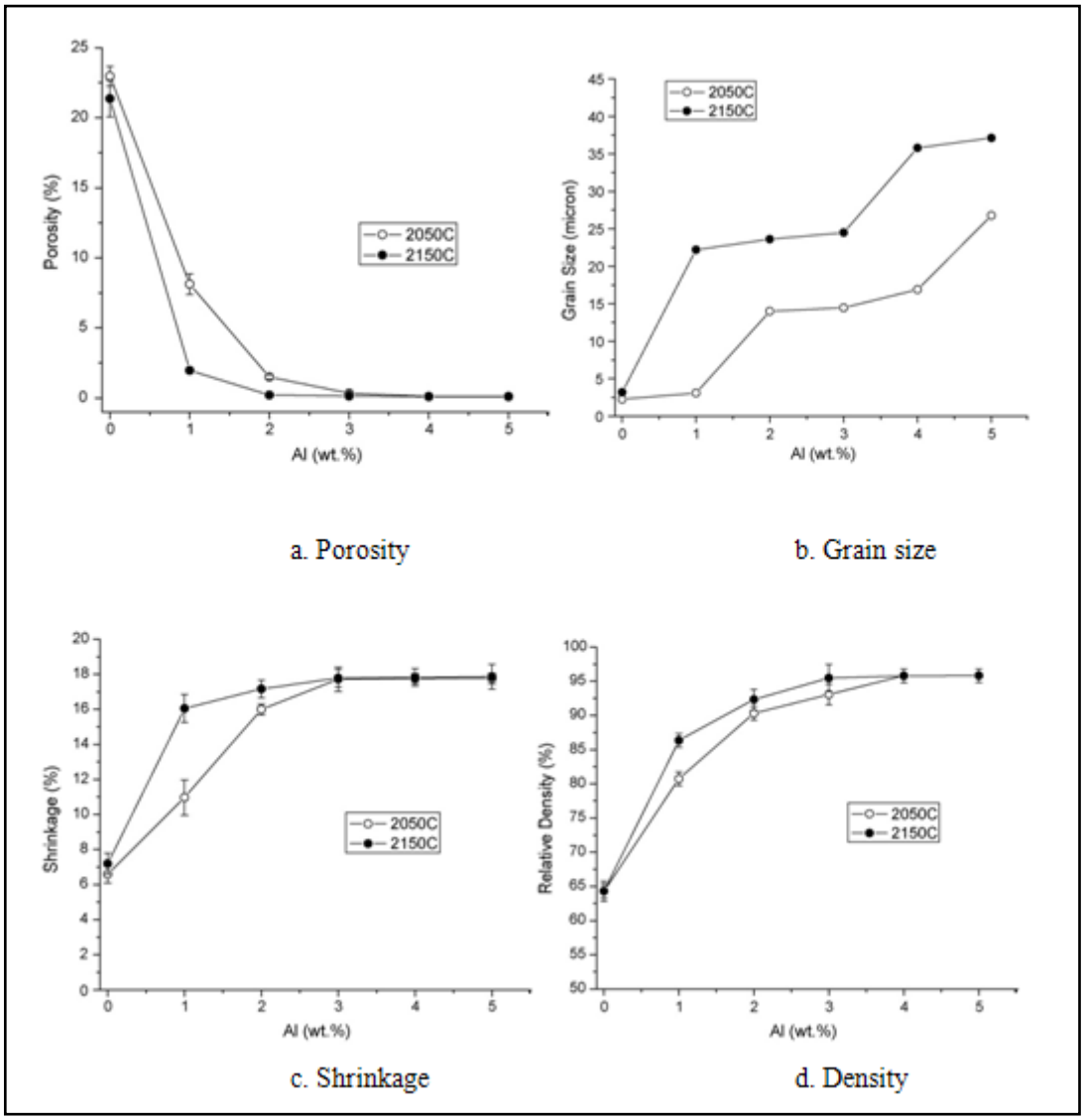

Figure 2.5. (a) Porosity (b) Grain size (c) Shrinkage (d) Density [19]

Onoro and friends studies the mechanical properties of particulate reinforced metal matrix composites based on aluminum alloys (6061 and 7015) at high temperatures. Boron carbide particles were used as reinforcement. All composites were produced by hot extrusion.

The particles were spherical in shape and less than 75µm in diameter. The diameters of B_4C were in range 8-10µm. The aluminum alloy powders blended with 5wt%B_4C were mixed in a planetary ball. They were mechanically milled for 12 min at 150 rpm, Argon was used as the atmosphere during the milling. The mixing powders were die pressed at 200 MPa in cylinders that were 25 mm diameter.

The hardness measured, microstructure, the tensile properties and fracture analysis of these materials were investigated at room temperature to determine their ultimate strength and strain to failure. The fracture surface was analyzed by scanning electron microscopy [20].

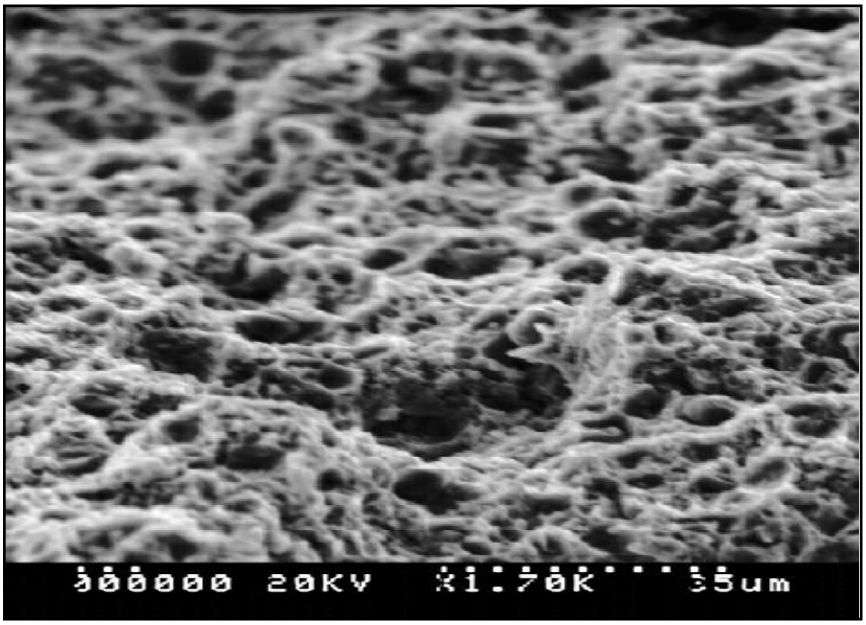

Figure 2.6. The sintered 6061 AMC with B4C ductile fracture at 20^0 C

An improvement in the mechanical behavior was achieved by adding B_4C particles as reinforcement in both matrix alloys.

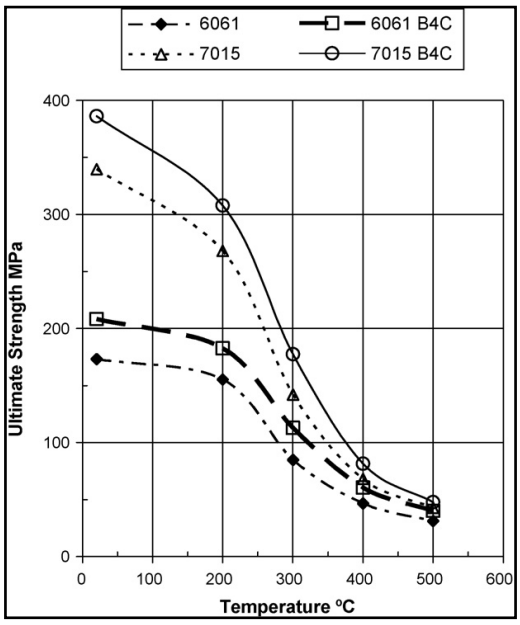

Figure 2.7. Tensile strength, the temperature of the sintered AMCs [20]

The tensile strength of AMCs with B_4C and aluminum 6061 and 7015 matrix alloys without reinforcing, decreased as the temperature increased. The ductility quantified in terms of elongation to failure and reduction in area increased as the test temperature increased.

Macroscopic observation of AMCs at room temperature revealed the fracture surface to be brittle [20].

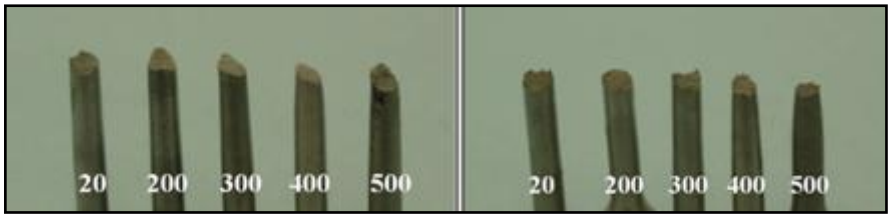

Figure 2.8. The sintered 6061 AMC with B4C particles [20]

Kerti and her friend studied microstructure variations in cast B_4C reinforced aluminum matrix composites (AMCs).In this study introduces a cost-effective and reliable casting technique to overcome the wetting problem between B_4C and liquid aluminum metal as well as the formation of undesirable phases at the interface using K_2TiF_6 flux .It was shown that B_4C addition with bigger particle size resulted in better microstructure with free agglomerated particles. Boron carbide powders of two different sizes used in this study. The particle sizes were <10, and >20µm.In order to enhance the wettabbility of boron carbide powders and improve their incorporation behavior into aluminum melts, potassium fluotitanate (K_2TiF_6) flux.

Different B_4C particulate reinforced AMCs were produced using 500 g of available aluminum charges which were melted in a SiC crucible utilizing induction furnace for each specimen. Mixture of B4C particles and the same amount of K_2TiF_6 flux were added into melt in the crucible. Finally the melt was poured into a metal mould. Microstructures were examined under the SEM equipped with EDX analysis.

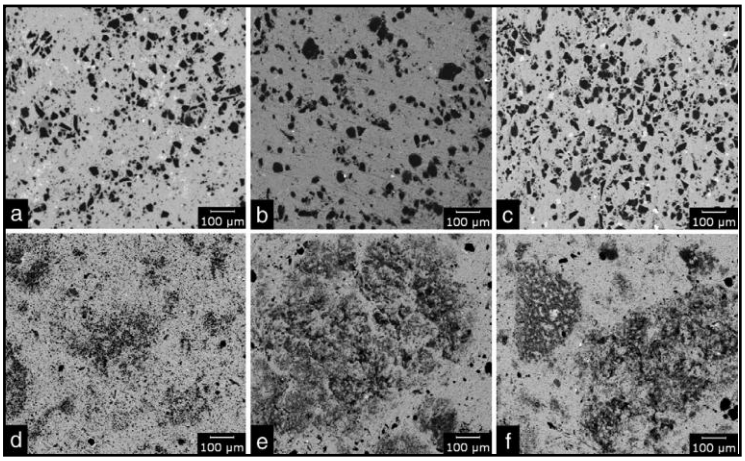

Figure 2.9. SEM images indicating that homogenous distribution of bigger B_4C_p

Finally, it is possible to produce Al-B_4C composites with homogenous microstructure using K_2TiF_6 flux by casting method. The amount of flux should be at least equal to the amount of B_4C particles, and it should be increased in the case of using particles which have higher particle ratios or smaller particle sizes. It has been concluded that the case of higher particle ratios and bigger particle sizes the holding time was not

enough to cover all of the particles with a reaction layer because of the agglomerated Ti compounds within the matrix. Addition of B_4C particles with bigger particle size results in more homogenous composite microstructure compared to the composite samples containing smaller particle size of B_4C due to agglomeration [21].

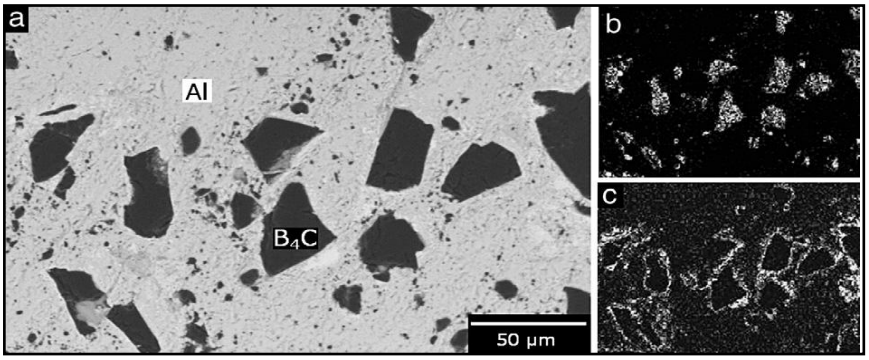

Figure 2.10. SEM micrograph of the B_4C particles [21]

3. EXPERIMENTAL PROCEDURE

Making effective use of numerical data relating to experiments of the samples Takashito sampling method was chosen. It deals with all aspects of experiments. Selected samples are subset of the larger set. Each individual is chosen according to increasing percentage and increasing particle size.

Table 3.1. Selected specimens

Material B_4C	**3%**	**6%**	**9%**
Ø22mm		X	
Ø77mm	X	X	X
Ø120mm		X	

3.1. POWDER CHARACTERIZATION

The powders were characterized for their size morphology and densities. Most characterization techniques require only a small quantity of powder. Boron carbide powders are used for the experiments. The characterization techniques used in the present study have been described in the following sections.

3.1.1. Powder Size

Powder size and size distribution was determined by using a laser scattering analyzer. (Malvern Mastersizer 2000 MV). Showed in Figure 3.1[22].

Figure 3.1. Laser analyzer machine at Yildiz Technical University

For determination of powder particle size distribution used laser diffraction and sampling method. Laser scattering is a streaming technique. In this study the particles are dispersed in a moving liquid stream. A few gram sample was adequate. Approxiametely one liters of water put into the sample chamber. Since the technique uses mixed water, laser beam, optics, dedector, and anolog-digital converter. This converter transferred to the computer as quantative via the special software and then particle size are calculated depends on the volume of particle size not weight. The particle analyzer was checked by measuring particle size of standard boron carbide.

Three measurements were made for each powder for statistically accurate results and the values were reported on graphics.

The measured particle sizes graphics by laser analyzer method are given in Figure 3.2 - 3.4.

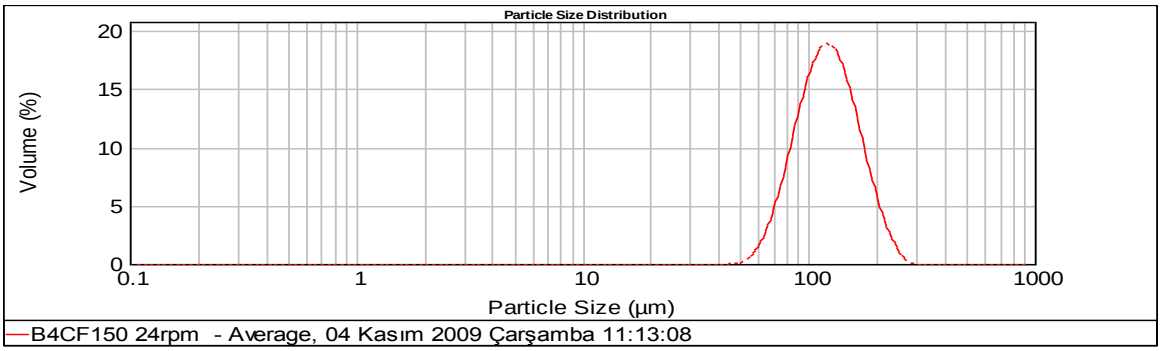

Figure 3.2. Particle sizes graphics of B_4C 150

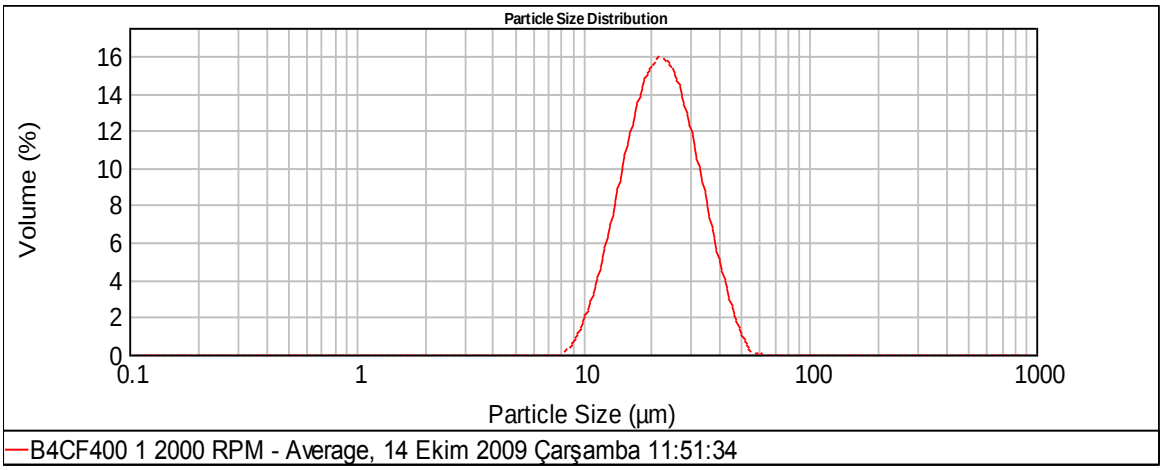

Figure 3.3. Particle sizes graphics of B_4C 220

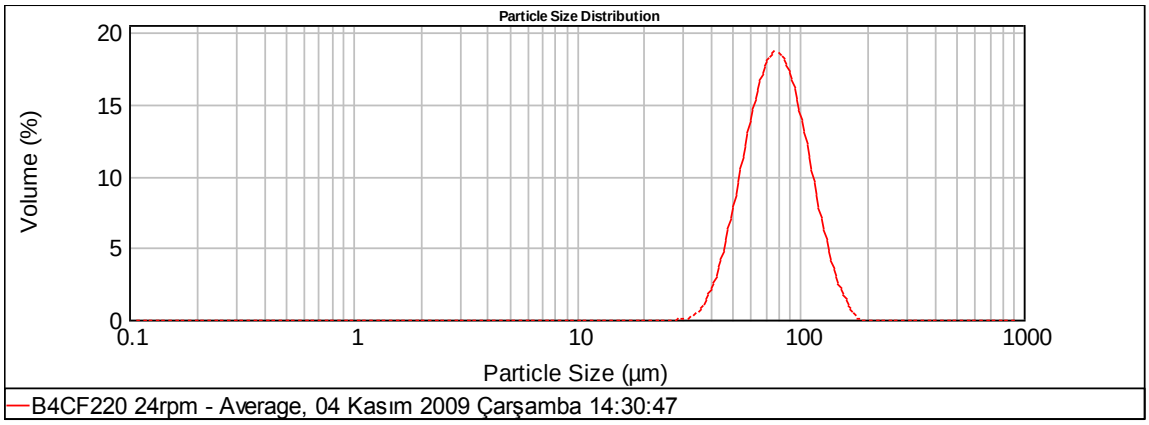

Figure 3.4. Particle sizes graphics of B_4C 400

3.2. POWDER PREPARATION

The powders need to be mixed, compacted and sintered .The usage techniques are discussed below.

3.2.1. Powder Mixing

Powders were weighed accurately and mixed with different amounts of elemental boron carbide (3, 6, and 9 wt%) to make up the final composition. The powders were weighed with an accuracy of 0.001 gram using an analytical balance. Weighed powders were placed in a twin shell (Figure 3.2) for one hour at 90 rpm Which imparted sufficient energy for the powder. This mechanism give diffusion intermixing of the particles. for the powder to mix homogenously.

Figure 3.5. Twin shell mixer at Ege University

Friction is the problem between the die wall and the powder during pressing. In this study zinc stearate lubricant wt 1% were used to minimize the die wear and easy ejection.

3.2.2. Compaction

For pressing single-ended compaction system was used. Test samples were determined Ø 10 mm in diameter and 60 mm in length. Pressure was 48 MPa. However under the applied load die was bent. The samples were sintered in 550 ºC. During sintering all the samples disintegrated. It should be noted that 48 MPa applied pressure was much lower than recommended pressure.

Figure 3.6. Manuel press and preliminary die

In the next step a new die designed and Mohr & Federhaff HFD10 Model uniaxial press was used. It is shown in Figure 3.4.

Figure 3.7. Uniaxial press at Yildiz Technical University

The samples were prepared in a cylindrical die Shown in Figure 3.5.

Figure 3.8. Cylindrical die

Samples sizes were Ø 10mm in diameter and 60 mm in length and compressed pressure was 445 MPa. All samples were cold pressed.

3.2.3. Sintering

The green parts sintered in a horizontal type sintering furnace. The chosen sintering furnace model is PTF 15/50/610. Figure 3.6. shows the sintering furnace

Figure 3.9. Sintering furnace at Yildiz Technical University

The sintered temperature was chosen at 550 ^{0}C .In powder systems with multiple components, the sintering process should be arranged according to the compound with the

lowest melting point. The melting point is 600 ^{0}C for aluminum, and 2350 ^{0}C for boron carbide

The sintering process took place in four stages

- Waiting period of fifteen minutes at 150°C
- Waiting period of fifteen minutes at 300°C
- Waiting process of fifteen minutes at 450°C
- The last period of sixteen hours at 550°C

The sintering was formed in argon atmosphere gas flowed rate of the furnace during sintering cycle. The heating process is shown in Figure 3.7.

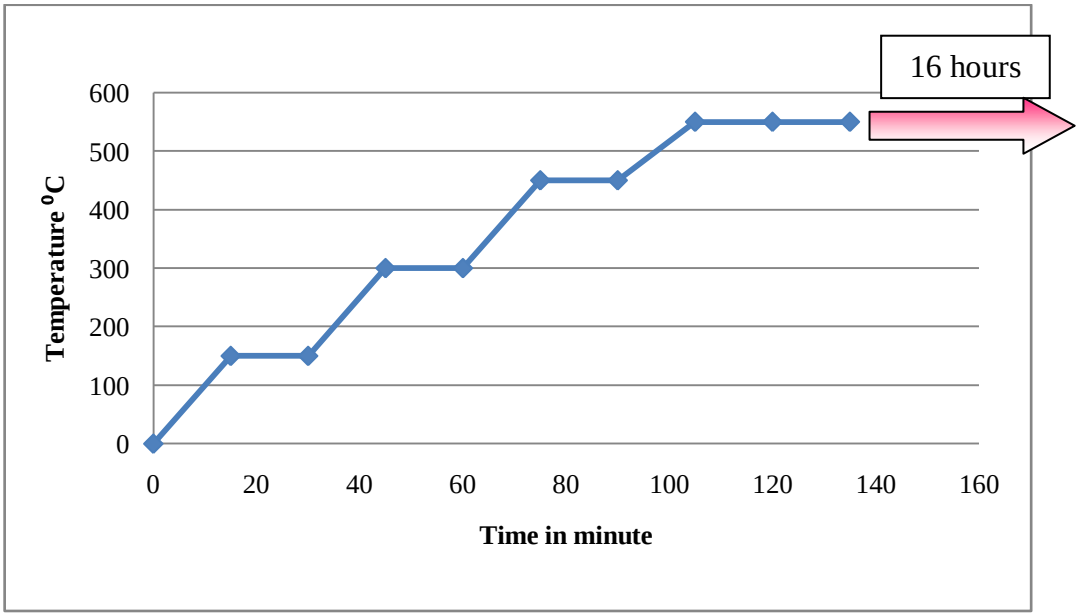

Figure 3.10. Heat treatment schedule

3.3. METALLOGRAPHY

Standard metallographic techniques were employed for preparing samples for micro structural examination. Metallographic samples were prepared from the widthwise cross-sections of the investigated composites. All samples were gently grinded with MD-piano

trademark 120, 220, and 1200 mesh emery papers. For grinding the sintered samples, Stuers Brand Grinding Machine was used. It is shown in Figure 3.8.

Figure 3.11. Stuers grinding machine at Yildiz Technical University

Afterwards samples were gently polished. For polishing diamond paste was used.

Figure 3.12. Stuers diamond paste and polishing cloths [17]

The polishing procedure involves polishing using 9µm diamond spray, followed by 6, 3, and 1 µm. After polishing all the samples were cleaned in pure alcohol and air dried.

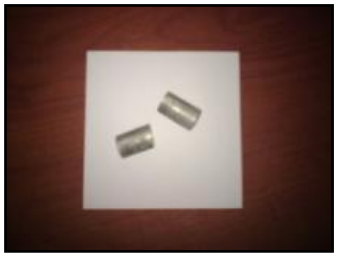

Figure 3.13. Samples

3.4. ELECTRON MICROSCOPY

The images were obtained by using Zeiss Evo 40 model Scanning electron microscopy (SEM) [23] The usage SEM machine is shown in Figure 3.10.

Figure 3.14. SEM machine at Yeditepe University

For investigation 6 Samples were chosen. At least four images were taken for each sample.

Table 3.2. Material numbers for experimental studies

Material number	Material name	Percentage (%)
1	Al-B_4CØ22	3
2	Al-B_4CØ22	6
3	Al-B_4CØ22	9
4	Al-B_4CØ120	3
5	Al-B_4CØ120	6
6	Al-B_4CØ120	9

Samples put in the device then vacuumed. Scanning samples were watched on the computer monitor and photographed. Backscattered electrons were used for Sem images. The samples were conductive for this reason they didn't coated with gold.

3.5. EDS- EDX (ENERGY DİSPERSİVE X-RAY SPECTROSCOPY)

Jeol Trade JSM 5910 SEM and Oxford Inca 7274 EDS was used to identify phases present in the samples. [24]. Quantitative data can also be obtained by comparing peak heights or areas in the unknown with standard material [25-26]. The chosen sample was Al-B_4C Ø77mm. That is exhibited in the Figure 3.11.

Figure 3.15. SEM and EDS machine at Marmara university

3.6. X-RAY DIFFRACTOMETER

Another qualitative analyze was applied by Tubitak .An automatic Shimadzu XRD-6000 diffractometer was used to identify phases present in the samples. The samples were polished and exposed to Cu X-ray tube (λ = 1.5405 Angstrom). Used sample was Al-B_4 C Ø77 6% [27].

Figure 3.16. Diffractometer

3.7. DENSITY

Density of the as received samples was measured using an analytical balance, shown in Figure 3.11.

Figure 3.17.Analytical balance

The samples were measured for their weight in air in 22°C at room temperature. They are measured for their weight in the water by the same machine with an added basket. The density calculation is based on Archimedes' principles on three randomly selected polished samples Distilled water was used as the immersion fluid. Densities of the samples was determined to an accuracy of 0.001 g/cm^3.

$$\rho\ (measured) = \frac{G\ air}{(Gair - Gwater)} \tag{3.1}$$

Where;

ρ $(measured)$ is density

$G\ water\ is$ weight in water

$G\ air\ is$ weight in air

The theoretical densities of materials were calculated assuming they were full-dense. The computation of theoretical density was carried out using rule of mixture as shown below

$$\rho_{th} = \rho_m V_m + \rho_f V_f \quad (3.2)$$

Where;

ρ_{th} is theoretical density of composite material (g/cm^3)
ρ_m is density of matrix material (g/cm^3)
ρ_f is density of reinforcement material, (g/cm^3)
V_m is volume fraction of matrix
V_f is volume fraction of reinforcement

The density of the samples was less than the theoretical value due to presence of internal porosity or impurities such as oxides. The other properties such as strength, stiffness can also be calculated in a similar manner. However in this study not calculated.

The porosity of composite material was calculated using the following equation.

$$Porosity = \frac{\rho_{th} - \rho_e}{\rho_{th} - \rho_a}. 100\% \quad (3.3)$$

Where;

ρ_e is experimental density (g/cm^3)
ρ_a is density of air (g/cm^3)

3.8. HARDNESS TESTING

Hardness measurements were carried out on polished samples using a Brinell hardness tester Reicherter mark BL-3 model hardness tester with a load 62.5 kg applied for 15 second. It is shown in Figure 3.12.

Figure 3.18. Hardness tester at Kosgeb laboratory

The two base diagonals of the ensuring pyramid were measured using a focal scale on the microscope of the testing machine. Calculation of the micro hardness value was based on the average length of the diagonals. Each hardness value was the average of four measurements. The presence of any subsurface particles and voids was identified by excessively high or low hardness values, respectively, and these values were also discarded.

3.9. COMPRESSION TESTING

The cylindrical samples were determined in accordance with ASTM test method B 925-08 [28] using Zwick Roel Model 2100 tensile testing machine with a 25.4 mm/min testing speed. The ends of a specimen should be flat and parallel [28-29]. In this study this requirement necessitated the machining and grinding of the ends of the specimens. However the length of the samples was less then the standard length. Test specimens that are to be tested in the compacting direction prepared from large sintered blanks into required dimensions by machining. Extensometer was not used for strain recording. The stress at 0.2% permanent offset was reported [28].

Figure 3.19. The testing machine at Siemens laboratory

Engineering stress-strain curves were obtained via computer programs using Standard methods.

3.10. RECRYSTALLIZATION (HEAT TREATMENT of SAMPLES)

The samples are recrystallized at 80 ºC about 15 min. This process made the deformed particles into the form of un deformed. After the compression testing all the compressed samples were recrystallized at 80°C [4], and compressed test performed again. Before and after all the compressed samples were photographed with TM 1000 Model Hitachi Mark SEM equipment at Kosgeb laboratory.

4. RESULTS AND DISCUSSION

4.1. MICROSTRUCTURAL EVOLUTION

Microstructural characterization studies were conducted on metallographically polished samples to investigate morphological characteristics of particles, and size and distribution of secondary phases. They were at various magnifications up to 20000 times. Microstructural investigation of samples after compression testing and recrystallization were also performed. Reveal micro structural features such as particle boundaries the evolution of microstructure after sintering of water atomized aluminum powder with 3%, 6% and 9% B_4C addition is shown Figure 4. 1-4. 6, respectively. The bright region represents the pure aluminum regions while black one as the B_4C particles. Figure 4.1 (a).

Decreasing size with increasing presence of B_4C fairly uniform distribution can be seen in Figure 4.1 (a), 4.2. (a) 4.3. (a) 4.4 (a) 4.5 (a) 4.6 (a).In the matrix there were no segregation and aggregation took place significantly. Interfacial integrity in terms of debonded regions and the presence of minimal porosity can be seen in Figure 4.4 (b) .This also been supported by the experimental porosity results obtained using density measurement Despite the fact that the bulks and the sizes of the phases arising in the interfaces are much smaller than the other phases. Results of micro structural characterization also revealed good interfacial integrity (ability of wetting) between B_4C and matrix (Figure 4.7) The images were obtained with backscattered electron photomicrographs of the specimen surface by using Zeiss Evo 40 model Scanning electron microscopy (SEM).

With increase in the weight percentage of B_4C the microstructure becomes more complex and phase accumulation along particle boundaries increases. Figure 4.8.

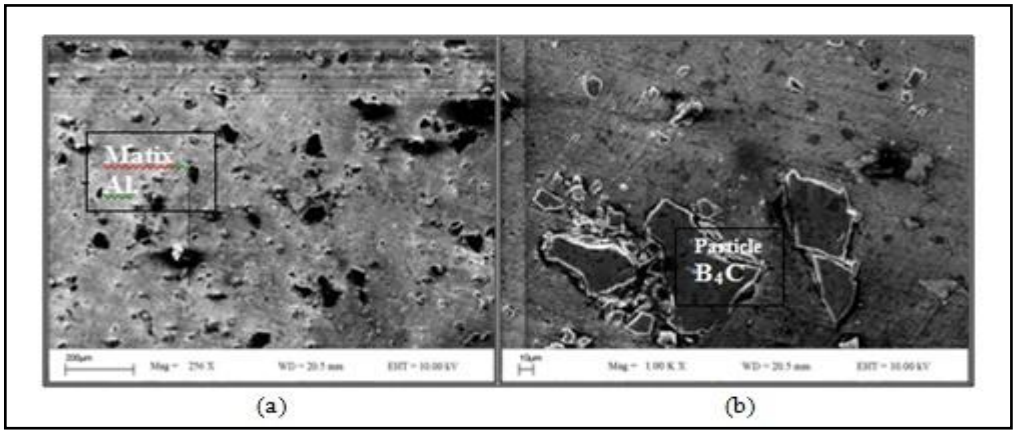

Figure 4.1. SEM micrographs for wt 9% Al-B_4C Ø22 (a) x 256 (b) x 1000

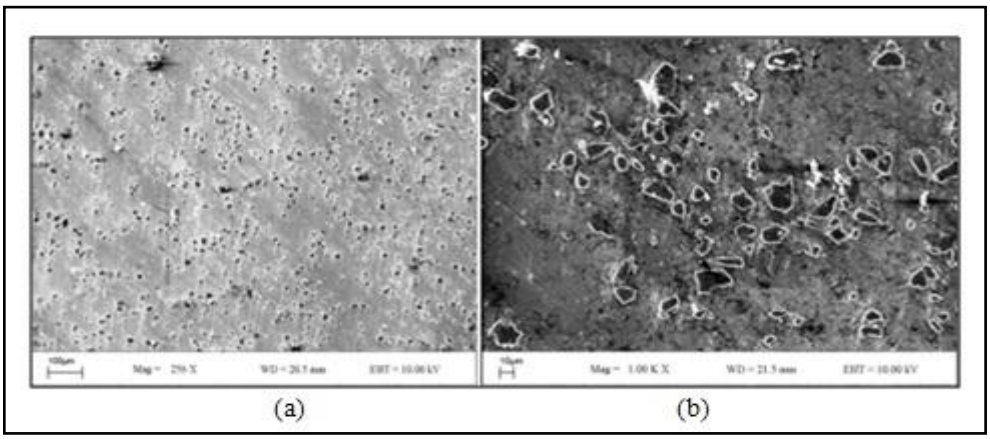

Figure 4.2. Sem micrographs for 6% Al-B_4C Ø22 (a) x 256 (b) x 1000

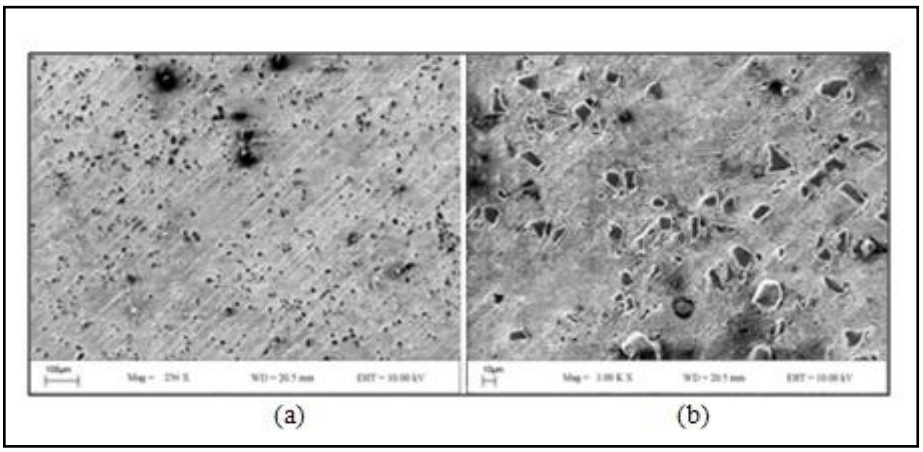

Figure 4.3. SEM micrographs for 3% Al-B_4C Ø22 (a) x 256 (b) x 1000

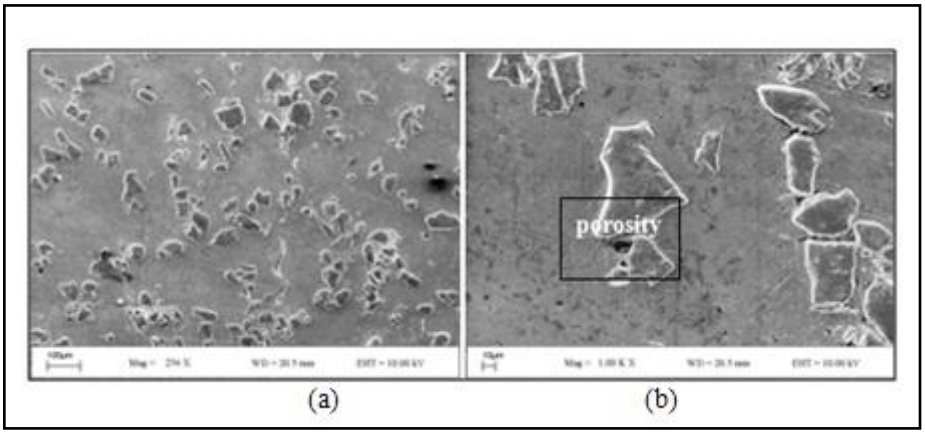

Figure 4.4. Sem micrographs for 9% Al-B_4C Ø120 (a) x 256 (b) x 1000

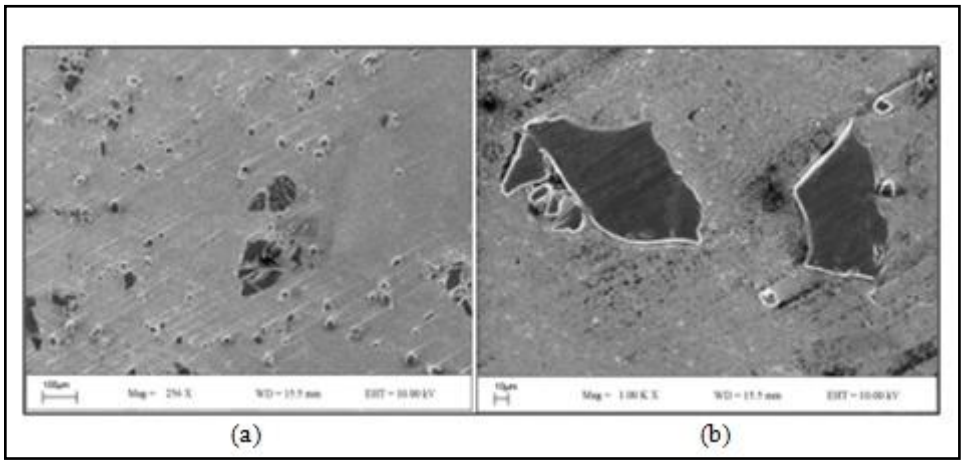

Figure 4.5. Sem micrographs for 6% Al-B_4C Ø120 (a) x 256 (b) x 1000

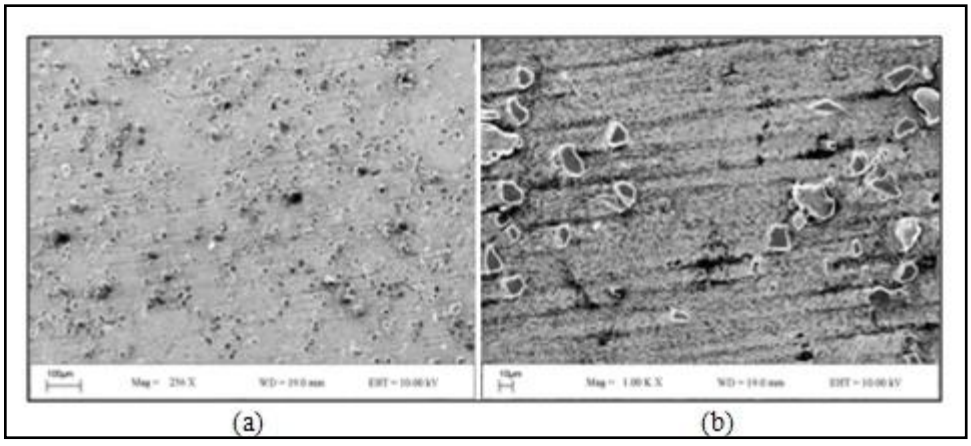

Figure 4.6. Sem micrographs for 3% Al-B_4C Ø120 (a) x 256 (b) x 1000

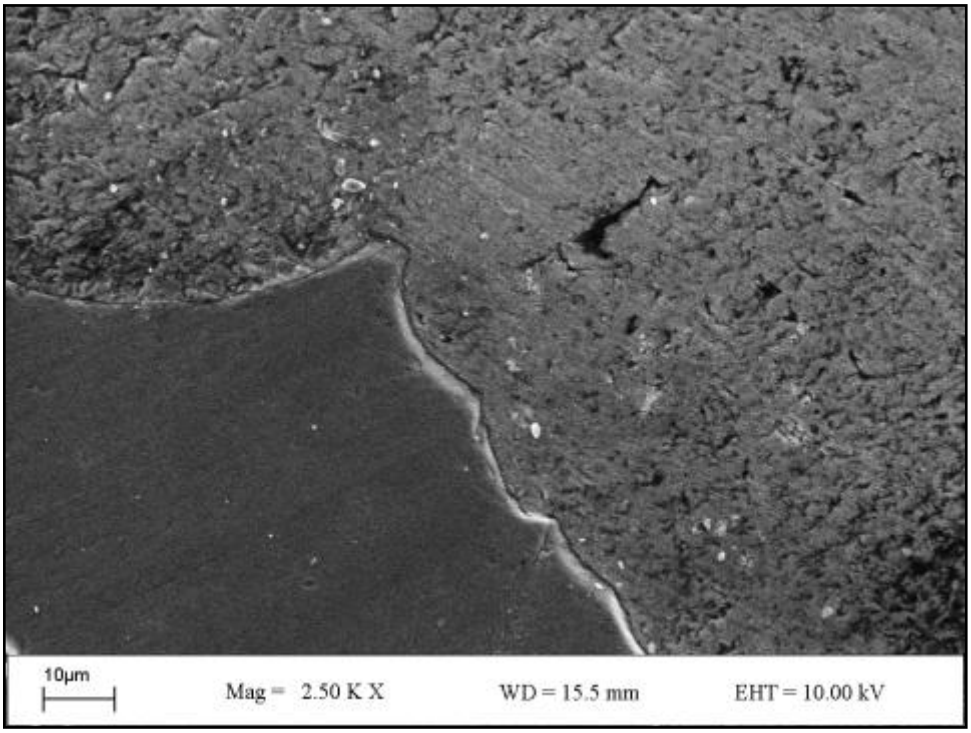

Figure 4.7.Fragtographs of Al-B_4C Ø22 6% sample

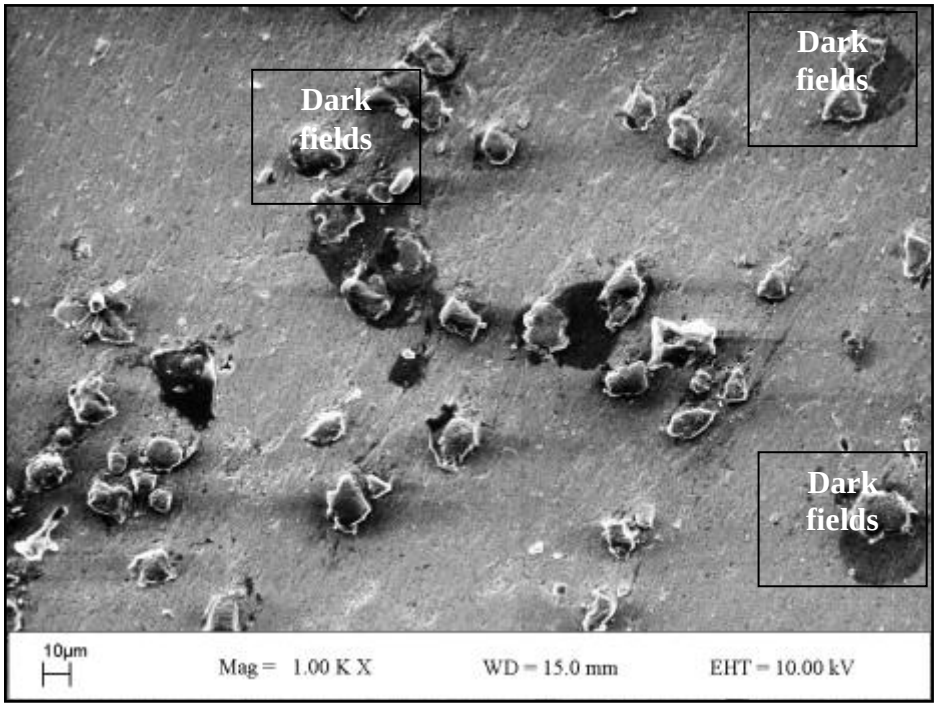

Figure 4.8. Fragtographs of Al-B_4C Ø22 9%

4.2. SEM and EDS ANALYSIS

Figure 4.9 shows microstructure of chosen sample Al-B_4C 6% Ø77mm. Energy dispersive spectrograph. Qualitative data obtained by comparing peak heights in the unknown with standard material. EDS revealed that all produced composites contained phases boron, aluminum, oxygen and iron.

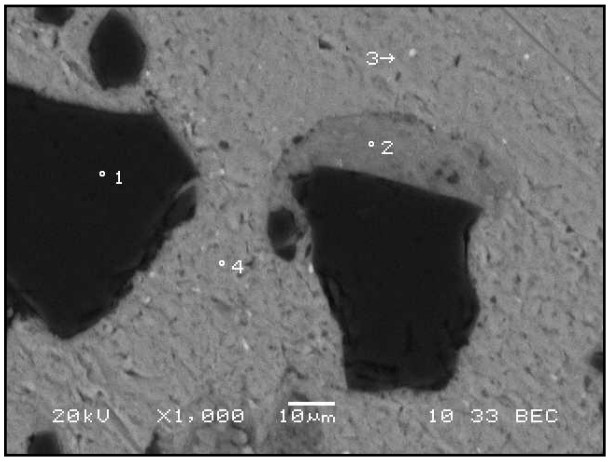

Figure 4.9. Al-B_4C Ø77mm 6% sem image

Figure 4.10 presents the EDS results of point one. The peak was identified Boron

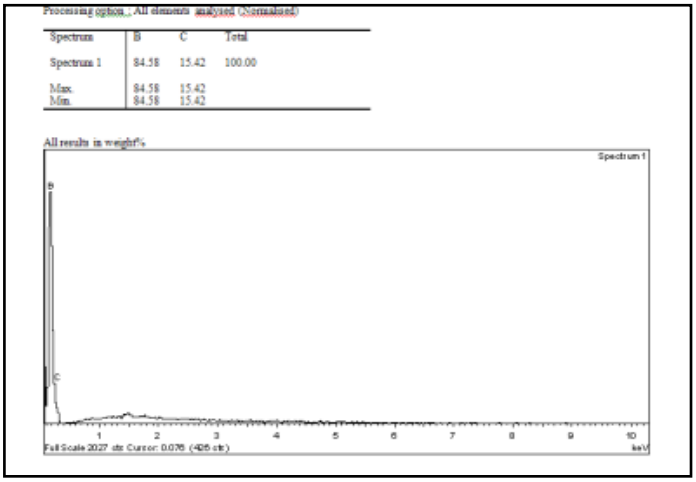

Figure 4.10. EDS pattern for Al-B_4C Ø77mm 6% point 1

Figure 4.11 presents the EDS results of point two. The peak was identified aluminum and oxygen. This point occurred due to the chemical activity of matrix and reinforcement compounds. Additionally the EDS peaks of sample in the grey color area was an intermetallic compound between the B_4C and aluminum occurred during sintering process.

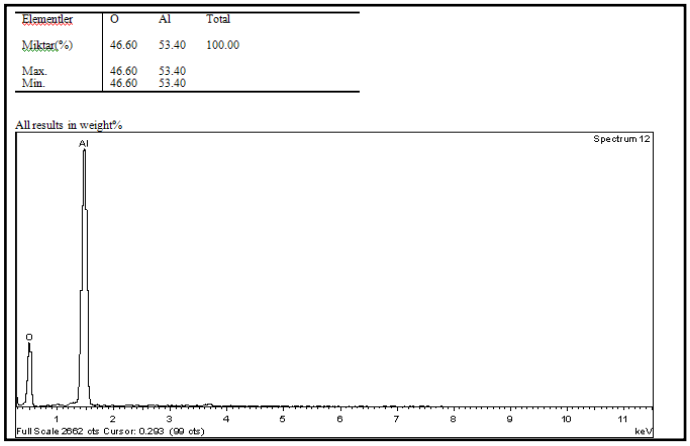

Figure 4.11. EDS pattern for Al-B_4C Ø77mm 6% point 2

Figure 4.12 presents the EDS results of point three. The peak was identified as iron. This compound was found in the peak precipitated by the grinding process.

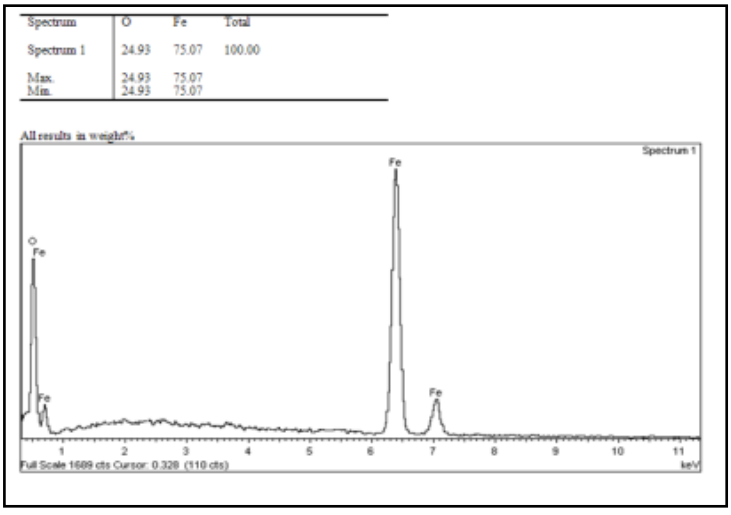

Figure 4.12. EDS pattern for Al-B_4C Ø77mm 6% point 3

4.13 presents the EDS results of point four. The peak was identified as aluminum in the sample and no other phases could be identified in the sample.

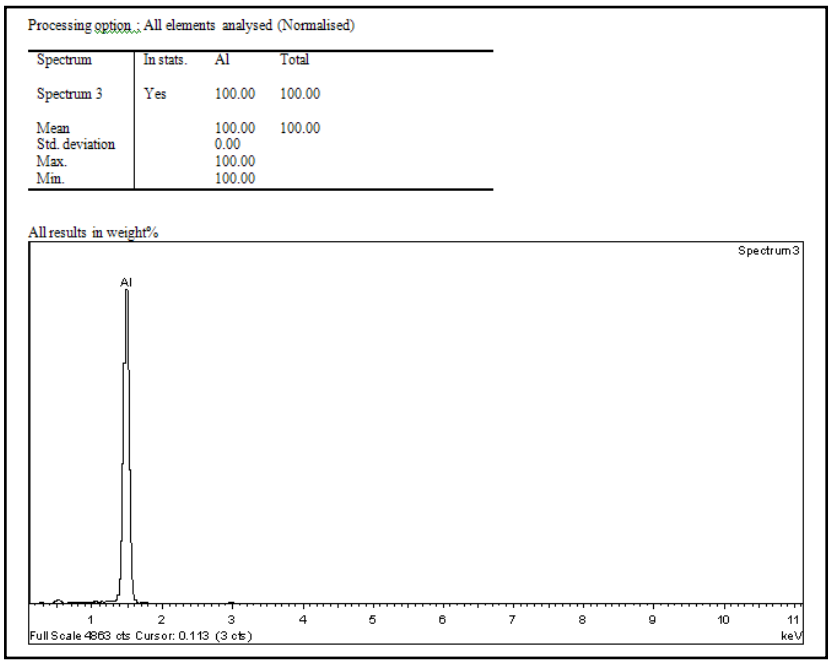

Figure 4.13. EDS pattern for Al-B4C Ø77mm 6% point 4

4.3. X-RAY DIFFRACTION

Figure 4.14 shows x-ray diffractgram obtained from Al-B_4C 6% Ø77 mm sample. Diffractgram shows the presence of intermetallic Aluminum boron AlB_2 and boron oxide B_2O. By using Cu X –ray tube ($\lambda = 1,5405\ A\ ngstrom$) Horizontal axis shows angle 2θ and versus intensity. The surface borided with B_4C powder shows peak of AlB_2 and B_2O.On the other hand the xrd graph of the surface alloyed with the peak of aluminum and B_4C.

*** Basic Data Process ***

Group : Endustriyel
Data : Al-B4C

Strongest 3 peaks

no.	peak no.	2Theta (deg)	d (A)	I/I1	FWHM (deg)	Intensity (Counts)	Integrated Int (Counts)
1	1	38.3086	2.34766	100	0.27410	2011	28924
2	2	44.5656	2.03150	61	0.21250	1234	15628
3	3	64.8445	1.43671	39	0.23820	780	10799

Peak Data List

peak no.	2Theta (deg)	d (A)	I/I1	FWHM (deg)	Intensity (Counts)	Integrated Int (Counts)
1	38.3086	2.34766	100	0.27410	2011	28924
2	44.5656	2.03150	61	0.21250	1234	15628
3	64.8445	1.43671	39	0.23820	780	10799
4	78.0409	1.22348	33	0.26030	654	9237
5	82.3085	1.17051	11	0.22290	215	2774
6	98.9924	1.01307	25	0.18050	506	4870
7	111.8801	0.92981	19	0.24760	380	5122
8	116.4151	0.90628	8	0.27630	163	2571

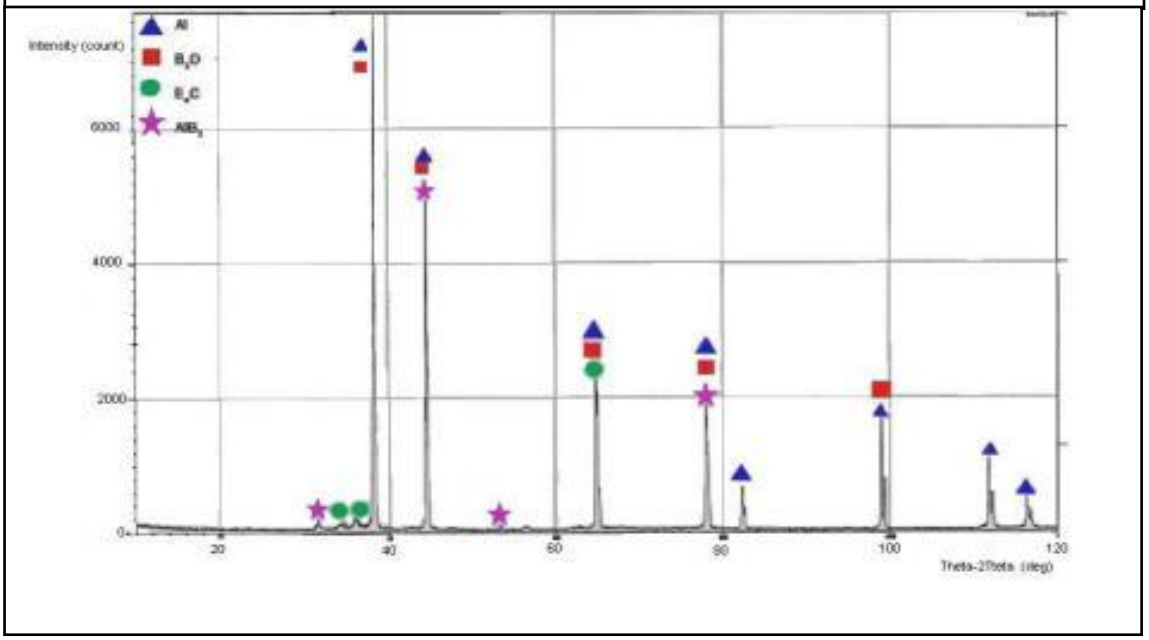

Figure 4.14. XRD pattern of Al-B_4C Ø77 6% material showing second phase.

4.4. DENSITY and POROSITY MEASUREMENT

The results of the density measurements are shown in Table 4.1.Table summarize the measured density and Table 4.2 estimated porosity of sintered aluminum matrix composite specimens containing 3%wt, 6%wt,and 9%wt B_4C reinforced material. The density of MMCs decreased from 2.69 g/cm^3 to 2.52 g/cm^3 as minimum with 3% B_4C Ø 77 reinforcement. Table 4.2 .By considering two extremities of the material such as Al and pure B_4C the density was expected to vary in between 2.69 g/cm^3 and 2.51 g/cm^3.This confirmed the continued existence of increasing density with increasing percentage of B_4C.

This is shown at a graphic in Figure 4.15 theoretically and in Figure 4.16 as measured densities. Also the porosity is observed approximately 5%. Pores caused by powder metallurgy manufacturing methods. The compressibility of the powder was related to the compaction pressure and compaction pressure was related with the density and porosity.

The biggest value was observed of Al-B_4C Ø 22 6% MMCs for density and Al-B_4C Ø 77 3% for the porosity. The increasing percentage of B_4C reinforcement was decreased the porosity.

Table 4.1. Measured weights and densities of the selected sample

Material	***Weight in air***	***Weight in water***	***Density***
Al-B_4CØ 120 6%	4. 0827	2. 4859	2. 5528
Al-B_4C Ø77 3%	3. 3132	2. 0046	2. 5270
Al-B_4CØ 77 6%	3. 8689	2.3601	2,.5590
Al-B_4C Ø77 9%	2. 8553	1. 7460	2.5706
Al-B_4C Ø22 6%	2. 5810	1.5806	2.5753

Table 4.2. Calculated porosities

Material	Theoretical density	Measured density	Volumetric porosity%
Al-B_4C Ø 1206%	2.6892	2.5528	5. 07
Al-B_4C Ø 77 3%	2. 6946	2. 527	6. 21
Al-B_4C Ø 77 6%	2. 6892	2. 559	4. 84
Al-B_4C Ø 77 9%	2. 6838	2. 5706	4. 21
Al-B_4C Ø 226%	2. 6892	2. 5753	4. 23

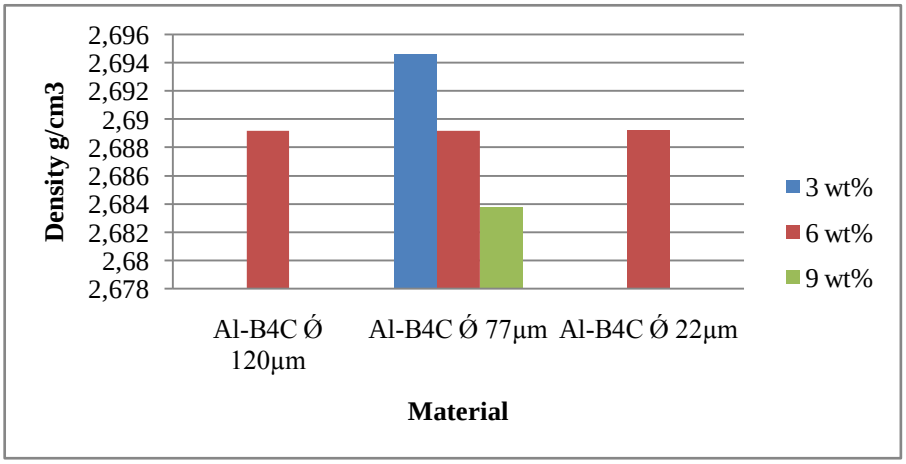

Figure 4.15. Theoretical densities of selected samples

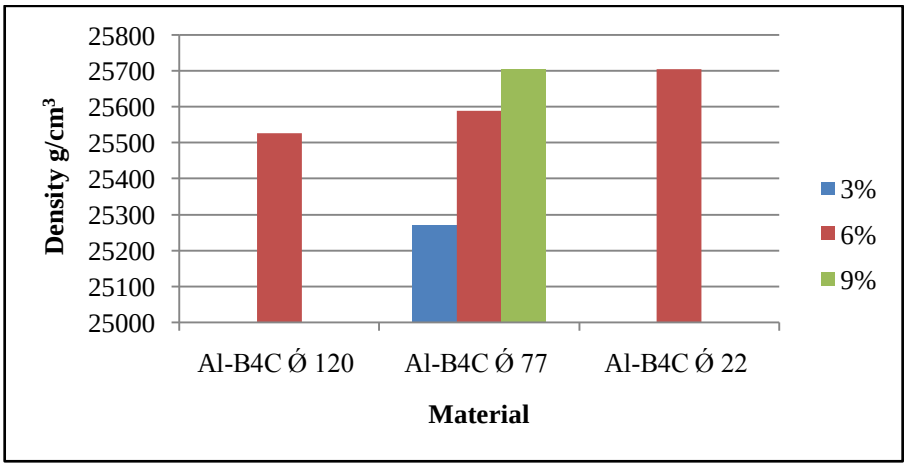

Figure 4.16. Measured densities of selected samples

When compared densities and porosities according Table 4.1 and 4.2 consequently, densities increased porosities decreased.

Table 4.3. Density and Hardness compared table

Material	**Density**	**HardnessHB before compressed**	**Hardness HB after compressed**
Al-B_4C Ø120	2.5528	24.75	30.25
Al-B_4C Ø77	2.5270	26.50	30.25
Al-B_4C Ø77	2.5590	25.75	32
Al-B_4C Ø77	2.5706	26.50	29.75
Al-B_4C Ø22	2.5753	26.25	39.75

Densities and porosities were related with the hardness value of the samples. When compared these values Al-B_4C Ø22 had the highest value of hardness and density.

About Mounting; samples embedded in resin to facilitate their handling and to improve the preparation result. Specimens that need perfect edge retention or protection of layers require mounting. All the samples cleaned prior to mounting for the surface free from Grease and other contaminants for the best possible adhesion of resin to sample.

Hot mounting is ideal for large numbers of samples coming to the lab successively. The resulting mounts will be of high quality, uniform size and shape and require a short process time and in general hot mounting resins are less expensive than cold mounting resins. For this reason Hot mounting techniques was chosen [30].

Figure 4.17. Samples in hot resin

A prominent increase in hardness was observed in composite samples when compared to pure aluminum material which has 15 Brinell hardness [31]. While making measurement the highest and lowest values were not taken into account, at least four points were measured for each sample.

The selected samples were Al powder reinforced with B_4C produced by powder metallurgy. The Brinell hardness method preferred because of contact area between metal surface are larger than the other methods.

The Brinell hardness tests have been carried out four different points. The average hardness values of the samples are listed at Table 4.5 and 4.6.

Matrix hardness were increased with decreasing B_4C particles diameters. This indicates that the dislocation in the matrix of the composite contribute to the increased of hardness. This result is in agreement with several other researchers [18, 3, 32, 33, 34].

Hardness is a measure of a materials resistance to plastic deformation. Plastic deformation corresponds to the braking of bonds with original atom neighbors and then reforming bonds with new neighbors [4].

Plastic deformation occurs, as with metals by the motion of dislocations. One reason for the hardness of these materials.

Effect of reinforcement particles on the hardness

Table 4.3 and 4.4 shows that the hardness of Al-B_4C MMC were increased with the reinforcements particles diameters.

Particle size of the reinforcement and the matrix and particle volume of the reinforcement and the matrix were influenced samples hardness. In this study general conclusions and their limits of the reinforcement role and its effect on hardness were investigated.

Table 4.4. Brinell hardness values after sintering

The Measured BHN Values from Different four Points for Each Pieces (before compressed)						
Material	**%B4C**	**the 1 st point**	**the 2nd point**	**the 3rd point**	**the 4 th point**	**Average**
Al-B_4C Ø 120	6	25	25	25	24	24.75
Al-B_4C Ø 77	3	27	27	26	26	26.50
Al-B_4C Ø 77	6	27	26	25	25	25.75
Al-B_4C Ø 77	9	27	27	26	26	26.50
Al-B_4C Ø 22	6	26	26	26	27	26.25

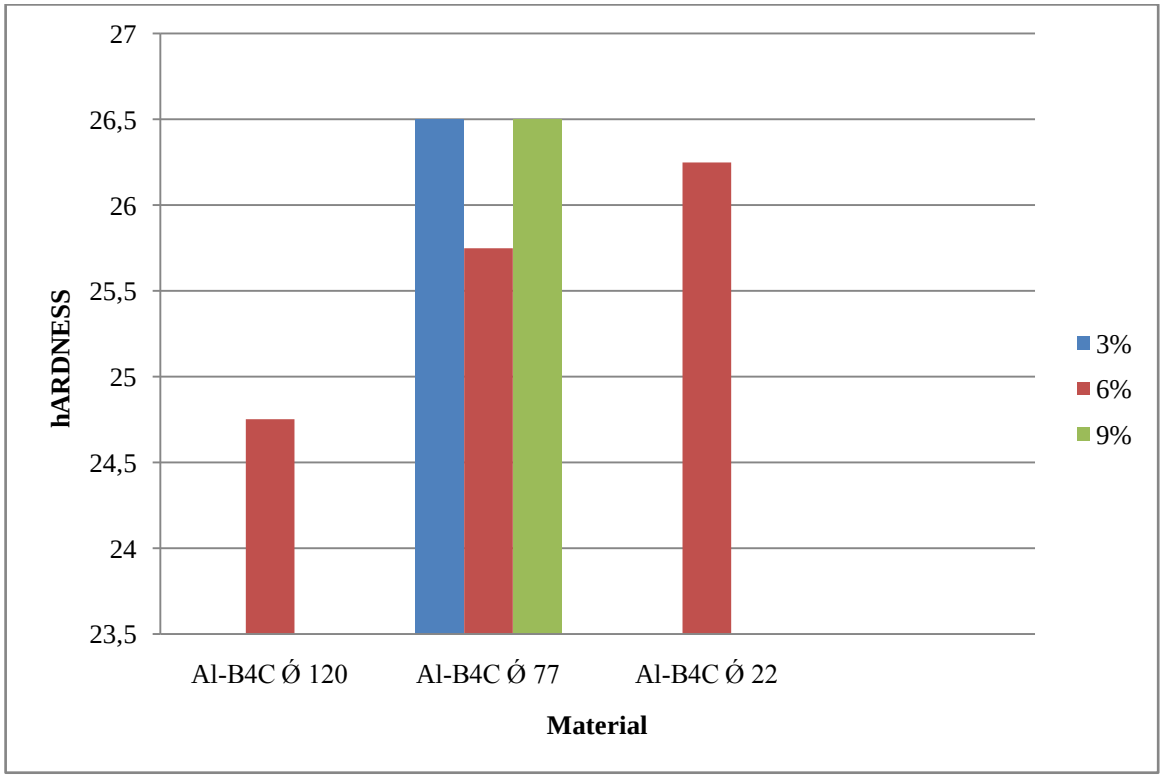

Figure 4.18. Brinell hardness values after sintering process

Table 4.5. Brinell hardness values after compressed

Material	**%B4C**	**the 1st point**	**the 2nd point**	**the 3rd point**	**the 4 th point**	**Average**
The Measured BHN Values from Different four Points for Each Pieces (after compressed)						
AlB_4CØ120	6	31	30	30	30	30.25
Al-B_4C Ø77	3	31	30	30	30	30.25
Al-B_4CØ 77	6	33	32	32	31	32.00
Al-B_4C Ø77	9	30	30	30	29	29.75
Al-B_4C Ø22	6	40	40	40	39	39.75

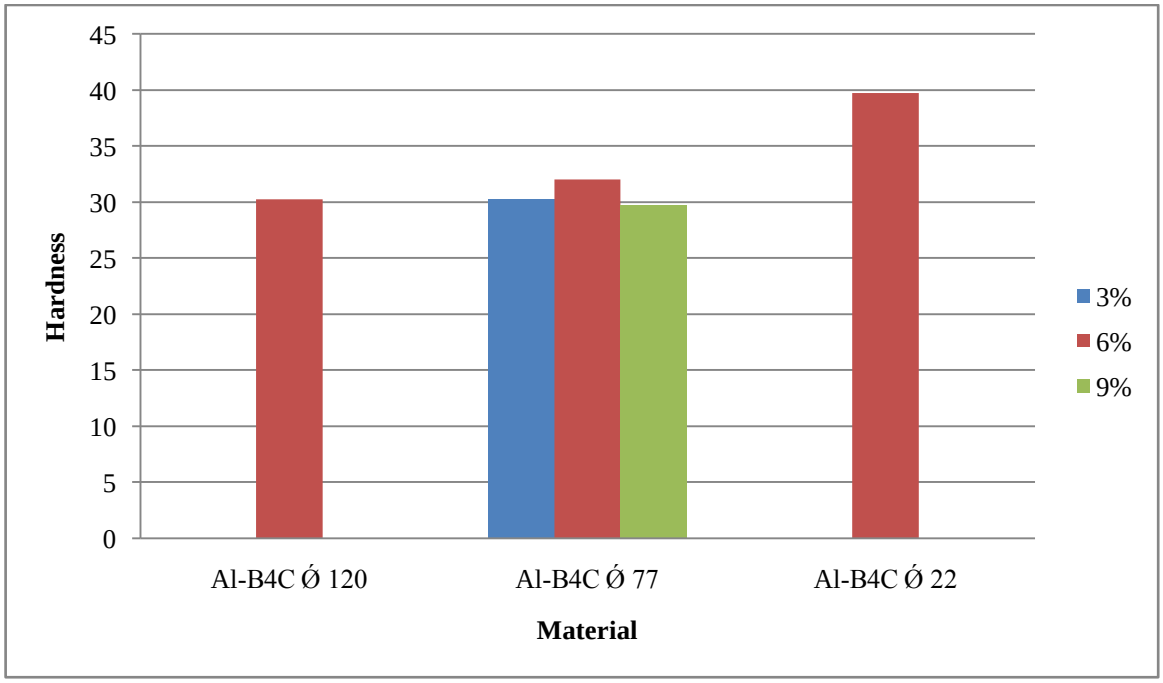

Figure 4.19. Brinell hardness values after compressed process

Increasing particle size of B_4C decreased the hardness of the composite. When the particles become smaller the particle boundary area per unit volume grew. This increased the slip resistance and plastic deformation becomes difficult. So hardness and stress increased.

When the size of reinforcing particles was approximately the size of the matrix particle ,the distribution of reinforcing particles in MMC had a substitution type [35].Sintering temperature chosen for the matrix materials. So, bonding strength at the interface between the two reinforcement particles during sintering would be weaker than the two matrix particles. Under stress the plastic deformation mechanism occurs as boundary slip which caused the decrease of the hardness.

4.6. COMPRESSIVE CHARACTERISTICS

The results of ambient temperature compression tests revealed a significant improvement in 0.2% yield strength (Figure 4.25) and ultimate compression strength of aluminum with an increase in amount of B_4C, but the ductility was compromised specially in the case of Al-B_4C Ø22 %9 samples. In addition of B_4C particles in Aluminum matrix led to simultaneous increase in strength levels Also, samples exhibited a significant increase in yield strength and elastic modulus when compared to monolithic aluminum yield strength 35 MPa [3]. But the noted that from the parameters elastic modulus not clearly observed. They are calculated from the slope approximately. Results are not reliable. Other techniques are available.

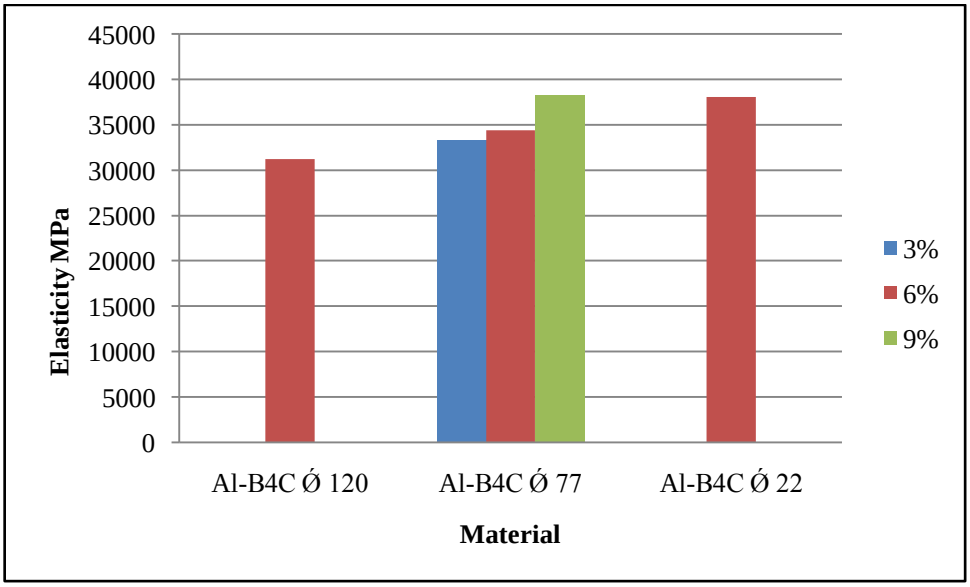

Figure 4.20. Modulus of elasticity

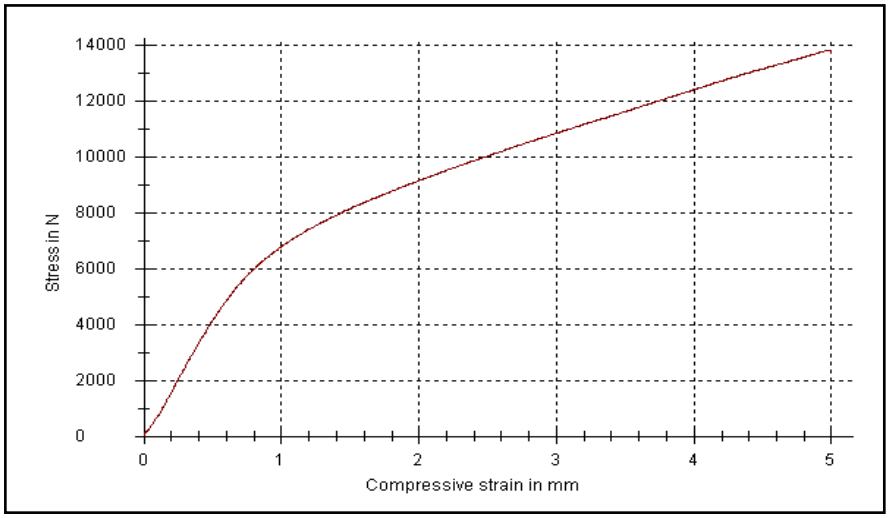

Figure 4.21. Compressive stress strain curves of Al-B_4C Ø77 µm % 3

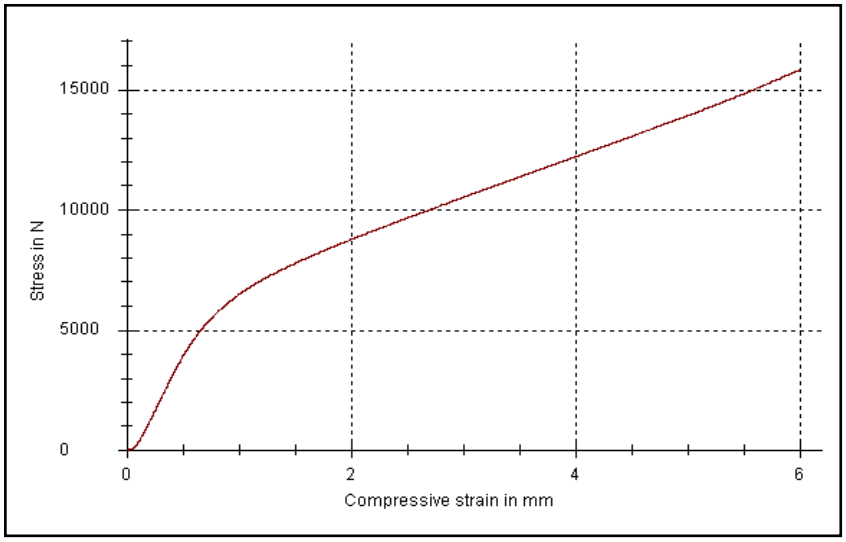

Figure 4.22. Compressive stress- strain curves of Al-B_4C Ø77µm % 6

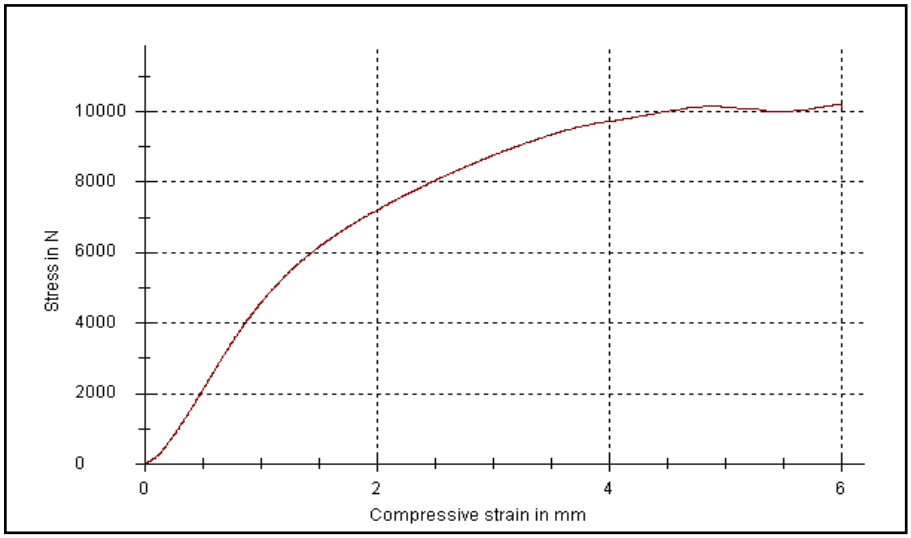

Figure 4.23. Compressive stress- strain curves of Al-B_4C Ø77 µm% 9

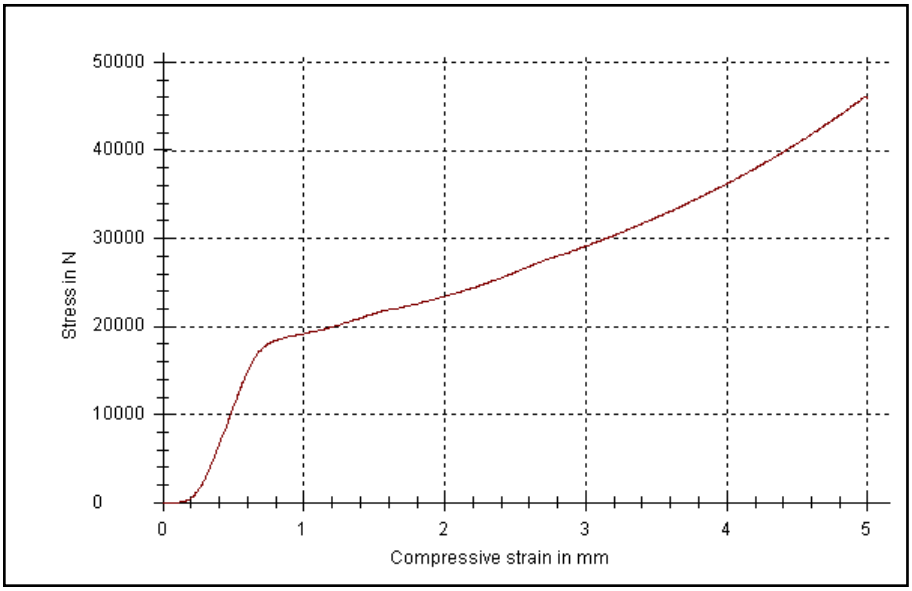

Figure 4.24. Compressive stress- strain curves of Al-B_4C Ø120 µm% 6

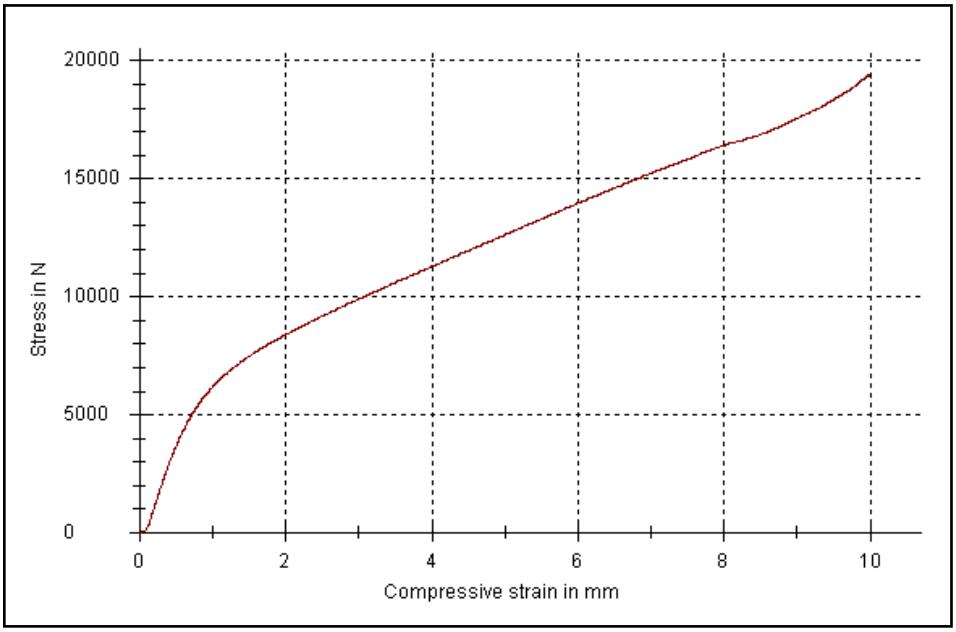

Figure 4.25. Compressive stress- strain curves of Al-B_4C Ø120 µm% 6

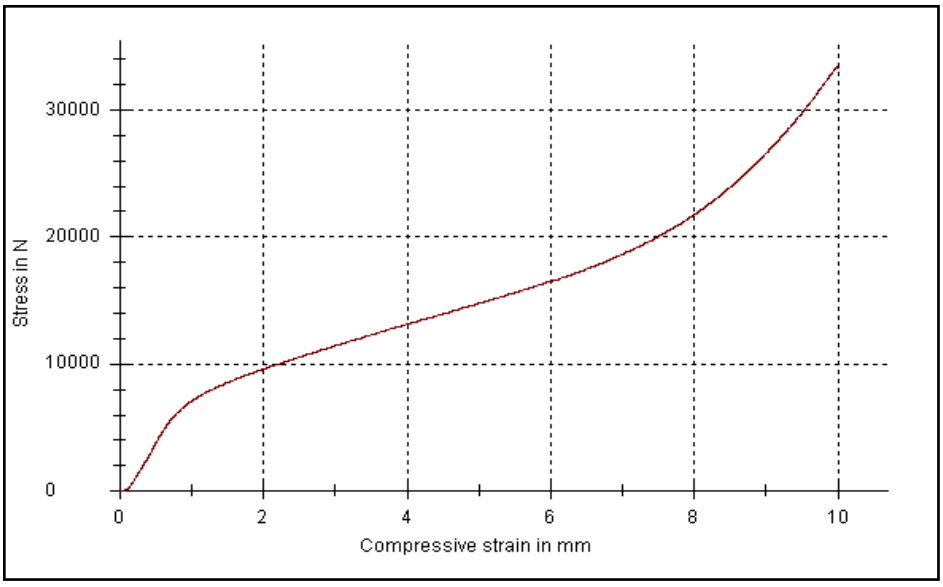

Figure 4.26. Compressive stress- strain curves of Al-B_4C Ø22µm % 6

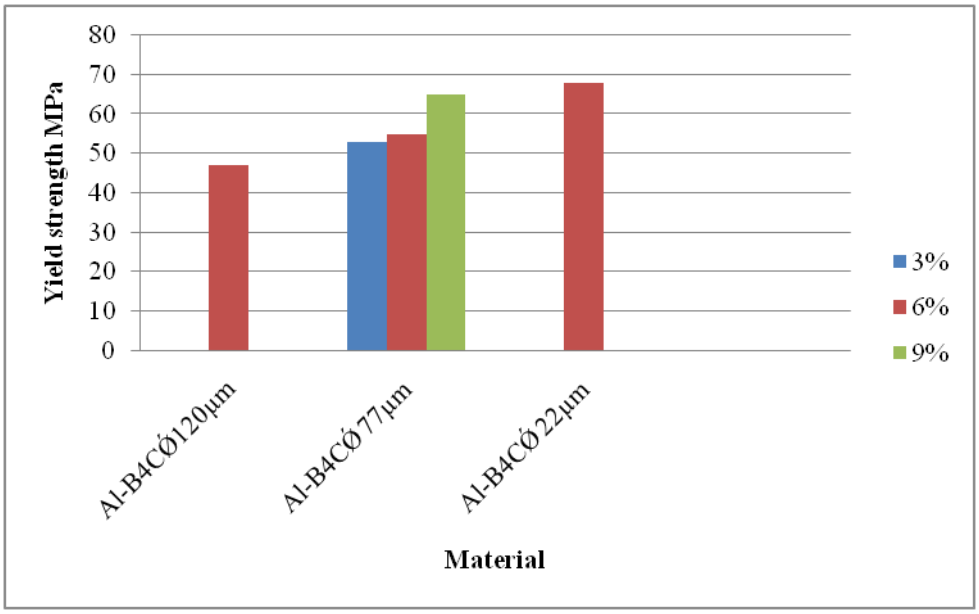

Figure 4.27. Yield strength graph

The bonding between Al-B_4C was weaker than the strength of bonding the aluminum matrix particles, moreover the magnitude of the weak interfaces were insufficient to cause "boundary slip" deformation. Thus the grain deformation mechanism dominates the plastic deformation behavior of Al-B_4C MMC with an increased B_4C contents. Under such conditions the B_4C particles restricted the plastic flow of the metal matrix and the Al-B_4C MMC was effectively strengthened [35].

4.7. DEFORMATION HARDENING EFFECT ON COMPRESSIVE STRENGTH

After compression test all the compressed samples recrystallized at 80 °C for fifteen minutes and then compression test performed again. Figures 4.26 and 4.27 show, before and after microstructural fragtograph of recrystallization samples by sem equipment.

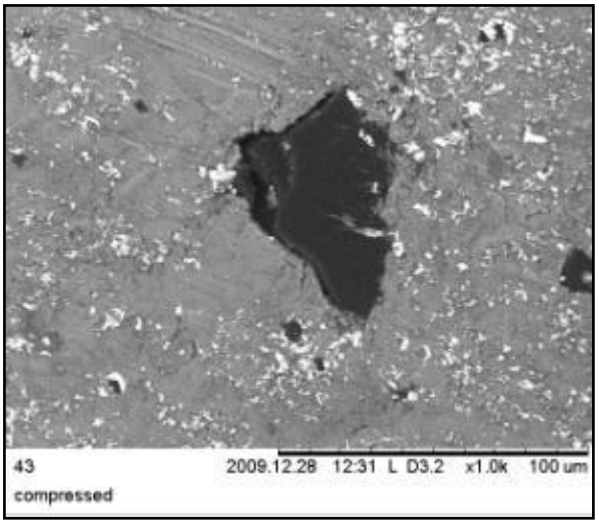

Figure 4.28. Al-B4C Ø77 %9 SEM images after compressed

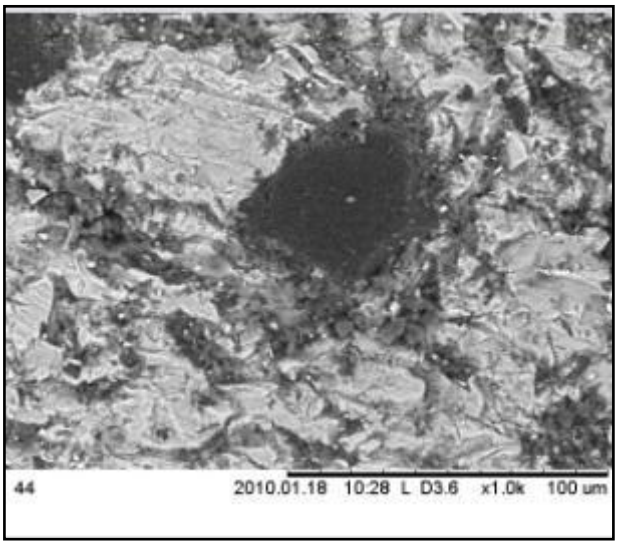

Figure 4.29. Al-B_4C Ø77 %9 SEM images after recrystallized

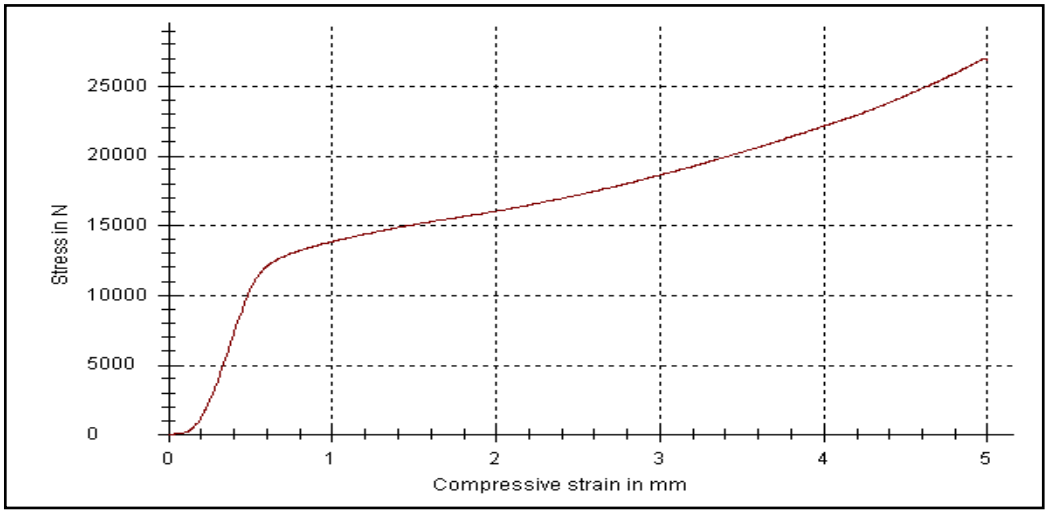

Figure 4.30. Compressive stress- strain curves of Al-B_4C Ø77 µm% 3

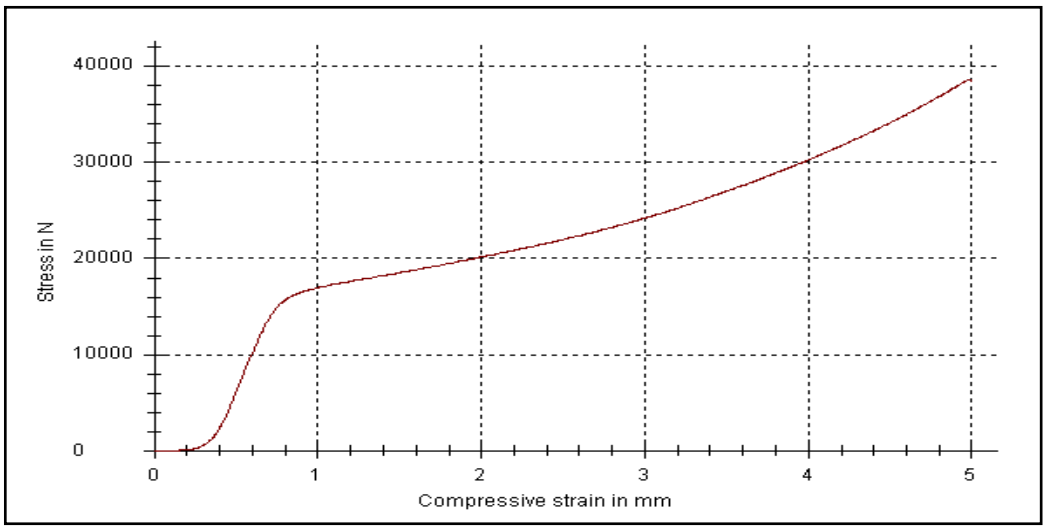

Figure 4.31. Compressive stress- strain curves of Al-B_4C Ø77 µm% 6

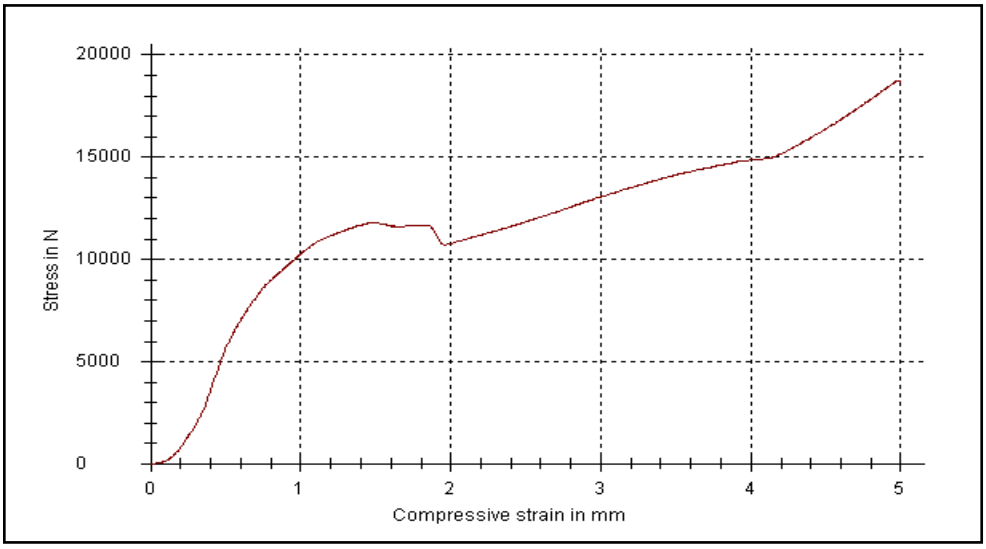

Figure 4.32. Compressive stress- strain curves of Al-B_4C Ø77 µm% 9

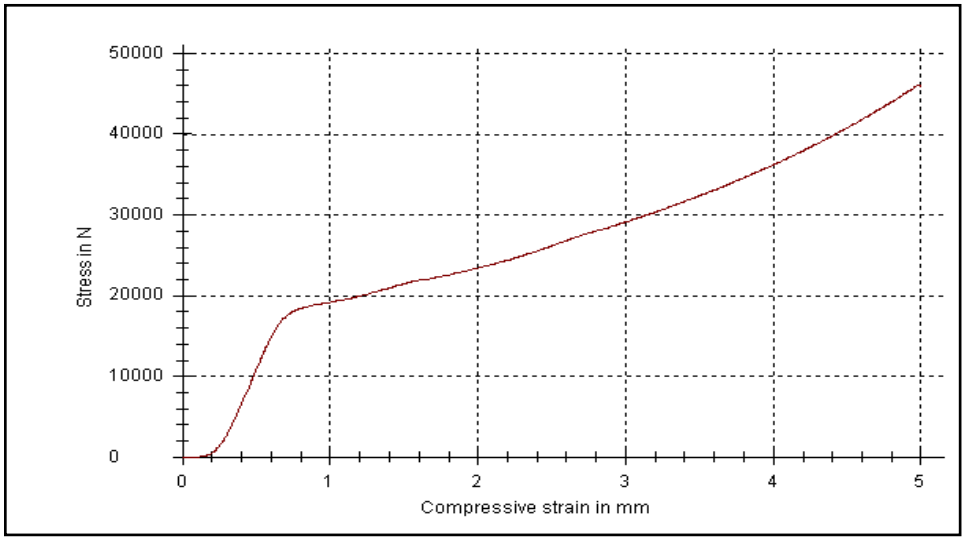

Figure 4.33. Compressive stress- strain curves of Al-B_4C Ø120 µm% 6

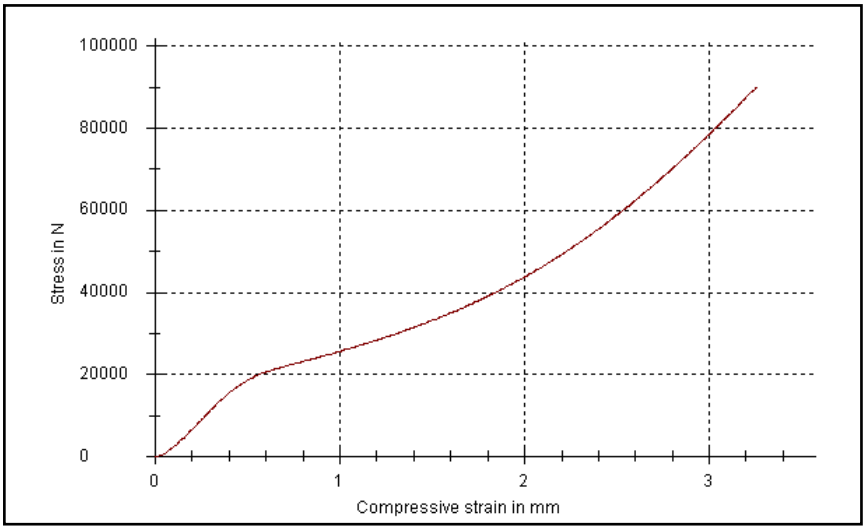

Figure 4.34. Compressive stress- strain curves of Al-B_4C Ø22 µm% 6

When compared before and after stress-strain curves the strengthening of al-B_4C MMCs by plastic deformation were observed. The strengthening occurred because of. dislocation movements within the crystal structure of material. After the primary compression test an increasing stress in required to produce additional plastic deformation and the metal become stronger and more difficult to deformed because of shear modulus.

The dislocation density was increased with the formation of new dislocations. The average distance of separation between dislocations decreased and dislocations were positioned closer together. On the average dislocation-dislocation strain interactions were repulsive. Motion of dislocation was hindered by the presence of other dislocations. As the dislocation density increased. Thus the stress of metal increased with the increasing hard working [4].

Al-B_4C with small particle size would strain harden more rapidly than the same compounds with a larger particle size.

5. CONCLUSION AND FUTURE WORKS

In this study for the increased trend of light-weight functional material in industrial applications, aluminum-boron carbide composites were selected. Pure aluminum composite reinforced with 3wt%-6wt% and 9wt% B_4C particles were used .Aluminum powders %99.5 purity, density 2.699 g/cm^3 with a nominal size of 63µm were used as a matrix material. All these materials were mixed in a twin-shell mixer at 90 rpm for one hour. The bonding material was zinc stearate added 1%.

In this study the particle sizes were measured with laser particle size measurement technique. The particle sizes were Ø 22 µm, Ø77 µm, Ø120µm for B_4C particles.

The tests samples were selected by Takashito sampling method

The densities were measured by Archimedes principle. The results are shown in table 4.3. .Theoretical densities were calculated according the formula (1.1). It can be seen easily densities are nearest the theoretical densities. The lowest value is Al- B_4C 3% Ø120 µm .The highest value is Al- B_4C 6 % Ø22 µm. The densities were increased when the particle size were decreased. However when reinforced percentage increased densities were linear increased. Smaller particle sizes decreased the porosities. Densities and porosities were related with the hardness value of the samples. When compared Table 4.3 Al-B_4C Ø22 had the highest value of hardness and density.

The hardness of the samples were measured by Brinell Hardness method because of this methods uses large measured area than the other methods, which perfected for P/M. Before measurements all the samples were put into the cold resin. The results are on the table 4.3. and 4.4. before and after compaction process respectively. The hardness values before compacting test were linear according the decreased particle size. For before compacting testing the highest value of the hardness was Al-Ø77µm B_4C 3-9% and the lowest value was Al--Ø120 µm B_4C 6%. The bigger particle size made the hardness lower. After the compacting testing increased the particle size made the hardness values less. The

lowest value was Al--Ø77 μm B_4C 9 % as 29,75 HB and the highest was Al--Ø 22 μm B_4C 6% as 39,75 HB.

When the reinforcing particles were approximately the size of the matrix particle, the distribution of reinforcing particles in MMC had a substitution type [35]. If the bonding between the reinforcing particles and the matrix particles was weaker than the strength of the matrix particles, then boundary slip occurred.

When the reinforced particles were much smaller than the matrix particles some reinforcements were present in the voids among the matrix particles. If the total volume of the reinforcements were less than the critical volume of voids, this result would cause the boundary of matrix particles well support and the deformation of these boundaries would be restricted. Finally, the strength of the composite increased Increasing particle size of B_4C decreased the hardness of the composite. When the particles become smaller the particle boundary area per unit volume grew. This increased the slip resistance and plastic deformation becomes difficult. So hardness and stress were increased.

Sintering process took four steps. Sintering time was chosen for 16 hours. Sintering temperatures and times were effective on the unwanted components. In this study sintering time took more than the previous studies. More time makes the unwanted components less. This is tested, and observed by the X-Ray analyst.

According the compressive tests the yield strength are shown in Figure 4.25. It can be seen easily that B_4C reinforced Al MMCs made the yield strength more when compared pure aluminum. The grain deformation mechanism dominates the plastic deformation behavior of Al-B_4C MMC with an increased B_4C contents. Under such conditions the B_4C particles restricted the plastic flow of the metal matrix and the Al-B_4C MMC was effectively strengthened [35]. The strength increased linearly according the particle size and percentages.

Particle size and volume was influenced elastic modulus test results. When look at the Figure 4.19. it is clear. Young modulus increased with the increased particle contents,

however decreased with the increased particle size. But noted that it was clearly, observed because of testing machines sensitive. Generally compacting test machines are not manufactured for the powder products testing. They are not perfect at the beginning strain sensitivity.

Deformation Hardening Effect on Compressive is, after recrystallization compressive test and hardness test performed again. The strengthening occurred because of. dislocation movements within the crystal structure of material. After the primary compression test an increasing stress in required to produce additional plastic deformation and the metal become stronger and more difficult to deformed because of shear modulus. So, hardness and strength were increased.

The following is list of topics recommended for future follow-up studies.

- Powder metallurgy advantages are ability to create complex shapes high strength properties, low material waste, eliminates or minimizes machining maintains close dimensional tolerances. So PM production methods in the near future and needs to concentrate this subject.

- Small amount of B_4C is effective in aluminum. This effectiveness will made the aluminum products kinds more for to produce machine elements.

- This thesis is based on compression tests and hardness tests. However, fracture test, thermal conductivity, fatigue test, plastic deformation and bending tests etc, needs to study

- Sintering temperature chosen at 550ºC .It can be change to the higher.

- For measurement the hardness there was not necessary put the samples in the resin.

- Some micrographs shows crashed particles for the reinforced materials. So, compression pressure can be decreased for powders during shaping process in the die. However can be increased for decrease the porosity.

- To investigate Boron and its derivatives develops the usage areas this metal. So, our sources will be evaluated.

REFERENCE

1. Chawla, K., *Composite Materials,* Springer Verlag, New York, 2001.

2. Jones,R.M., *Mechanics of Composite Materials,* Taylor & Francis, Philadelphia,1999.

3. Topcu,I., H. O. Gulsoy, N. Kadioglu., and A. N. Gulluoglu, "Journal of Alloys and Compounds", *Processing and mechanical properties of B_4C reinforced Al matrix composites,* 482, pp. 516-521, 2009.

4. Callister,W. D., *Materials Science and Engineering an Introduction,* John Wiley, USA, 2007.

5. Chawla, K., *Metal Matrix Composite,* Springer, USA, 2006.

6. Hull, D. and T. W. Clyne, *An Introduction to Composite Materials* Cambridge University, New York, 1985.

7. Ipek, R.,*Composite Materials* Lecture notes, 2000.

8. German, R.M., *Powder Metallurgy Science,* New Jersay, USA, 1997.

9. German, R.M., *Toz Metalurjisi ve Parçacıklı Malzeme İşlemleri*, Türk Toz Metalurjisi Derneği, Ankara, 2007.

10. Ipek, R., *Powder Metallurgy* Lecture Notes, 2000.

11. Metals Handbook., *Powder Metallurgy,* Vol. 7, ASM International Information Society, 1998.

12. Hall, E.J., *Process for Disintegrating Metal*, U.S.Patent 1,659,291, 14 Feb 1928.

13. ASM Specialty Handbook., *Aluminum and Aluminum Alloys,* ASM International Information Society, 1993.

14. Some Examples of Aluminum Powders, available on web site www.alcoa.com.

15. Luyk, K.E., *Aluminum,* American Society for Metals, 1967.

16. Rolles, R., *Aluminum Flake Pigment*, Pigment Handbook, John Wiley&Sons, New York, 1973.

17. Stuers diamond paste and polishing cloths, available on web site www.stuers.com.

18. Mohanty, R.M., K. Balasubramanian, and S.K.Seshadri.,*"*Materials Science and Engineering A", *Boron carbide reinforced aluminum 1100 composites fabrication and Properties,* G Model, MSA 24288, pp. 11, 2008.

19. Mashhadi, M., E.T.Nassaj., V.M.Sglavo., H.Sarpoolaky., Ehsani, N.,"Ceramics International 35", *Effect of Addition on Pressureless Sintering of B_4C,* pp. 831-837, 2009.

20. Onoro,J., M.D.Salvador., Cambronero,L., *"*Materials Science and Engineering A", High-temperature mechanical properties of aluminum alloys reinforced with boron carbide particles, Pp 421-426, 2009.

21. Kerti, I. and F.Toptan, "Science Direct", Microstructural variations in cast B_4C-reinforced aluminum matrix composites Materials Letters 62, pp. 1215-1218, 2008.

22. Laser scattering analyzer, available on website www.malvern.com.

23. Scanning electron microscopy (SEM) available on website www.Jeal.com/sem.

24. Jeol Trade JSM 5910 SEM and Oxford Inca 7274 EDS available on website www.mse.iastate.

25. Oxford Inca 7274 EDS available on website www.oxford-instruments.com.

26. Oxford Inca 7274 EDS available on website www.wikipedi.org/wiki/energy-dispersive.

27. Shimadzu diffractomete available on website www.x-raymicroanalysis.com .

28. ASTM standards E9-87 *Compression Testing of Metallic Material at Room Temperature*, ASTM international 2000.

29. Onaran, K., *Malzeme Bilimi*, Bilim Teknik Yayınevi, 2009.

30. ASTM Standards B925-08 *Compression Testing*, 2003.

31. Gürü, M., Yalçın, H., *Malzeme Bilgisi*, Palme Yayıncılık, Ankara, 2006.

32. Mondal, D.P., S.Das, Suresh,K.S and Ramakrishnan,N.,"Material Science and Engineering A" *Compressive deformation behavior of coarse SiC particle reinforced composite*,pp. 460-461, 550-560, 2007.

33. Jiang, Q.C., H.Y.Wang., B.X.Ma., Y.Wang., and F.Zhao., "Journal of Alloys and Compounds", *Fabrication of B_4C particulate reinforced magnesium matrix composite by powder metallurgy*, pp.177-181, 2005.

34. Gursoy,A.K. and A.Kalemtas, "Journal of the European Ceramic Society", *Processing of silicon carbide boron carbide aluminum composites*, pp 8, 2008.

35. Lin, Y.C., H.C.Li., S.S.Liou., and Shie, M.T., “Material Science and Engineering A”, *Mechanism of plastic deformation of powder metallurgy metal matrix composites of Cu-Sn/SiC under compressive stress*, pp.363-369, 2004.